

AUTOMATED DETECTION OF CONGESTIVE HEART FAILURE BASED ON THE EIGENVALUE DECOMPOSITION OF HRV SIGNALS

M.Tech. Thesis

By
ASHISH KUMAR



**DISCIPLINE OF ELECTRICAL ENGINEERING
INDIAN INSTITUTE OF TECHNOLOGY INDORE**

JUNE 2017

AUTOMATED DETECTION OF CONGESTIVE HEART FAILURE BASED ON THE EIGENVALUE DECOMPOSITION OF HRV SIGNALS

A THESIS

*Submitted in partial fulfillment of the
requirements for the award of the degree
of
Master of Technology*

by
ASHISH KUMAR



**DISCIPLINE OF ELECTRICAL ENGINEERING
INDIAN INSTITUTE OF TECHNOLOGY INDORE**

JUNE 2017



INDIAN INSTITUTE OF TECHNOLOGY INDORE

CANDIDATE'S DECLARATION

I hereby certify that the work which is being presented in the thesis entitled **AUTOMATED DETECTION OF CONGESTIVE HEART FAILURE BASED ON THE EIGENVALUE DECOMPOSITION OF HRV SIGNALS** in the partial fulfillment of the requirements for the award of the degree of **MASTER OF TECHNOLOGY** and submitted in the **DISCIPLINE OF ELECTRICAL ENGINEERING, Indian Institute of Technology Indore**, is an authentic record of my own work carried out during the time period from July, 2016 to June, 2017 under the supervision of Dr. Ram Bilas Pachori, Associate Professor, Discipline of Electrical Engineering, IIT Indore.

The matter presented in this thesis has not been submitted by me for the award of any other degree of this or any other institute.

**Signature of the student with date
(ASHISH KUMAR)**

This is to certify that the above statement made by the candidate is correct to the best of my knowledge.

**Signature of the Supervisor of with date
(Dr. Ram Bilas Pachori)**

ASHISH KUMAR has successfully given his M.Tech. Oral Examination held on **19-06-2017**.

Signature of Supervisor of M.Tech. thesis
Date:

Convener, DPGC
Date:

Signature of PSPC Member
Date:

Signature of PSPC Member
Date:

Acknowledgements

First of all, I would like to express my sincere gratitude to my thesis supervisor **Dr. Ram Bilas Pachori** for his constant support and guidance through the learning process of this master thesis. Furthermore, I would also like to express my gratitude to my PSPC committee members **Dr. Vivek Kanhangad** and **Dr. Anand Parey** for their valuable suggestions.

I would also like to thank all the faculty members and the staff at IIT Indore for their cooperation throughout my M.Tech degree. I would like to thank the Discipline of Electrical Engineering for providing all the facilities and resources required for the completion this work.

I would like to thank all the members of Signal Analysis Research Lab for their assistance during this work. In particular, I would like to thank Mr. Rishi Raj Sharma and Mr. Mohit Kumar for their assistance at various levels of this work.

I would also like to thank Mr. Praveen Singya, Mr. Vinay Bankey, and Mr. Ram Bansal for their invaluable support during my stay at IIT Indore.

I am grateful to my batchmates Anuj, Anish, Saurabh, Parual, Sushree, Khushbu, Neetu, Rituraj, Sandeep, Rampoojan, Ashima, and Gaurav for their support and making my stay at the institute enjoyable.

I am especially grateful to my family members for their invaluable support and strong belief in me.

ASHISH KUMAR

(mt1502102002)

M.Tech. (Communication and Signal Processing)

Discipline of Electrical Engineering, IIT Indore

Dedicated to My Parents

Abstract

Electrocardiogram (ECG) is a noninvasive diagnostic tool which is widely used to diagnose the cardiovascular diseases (CVD). Heart rate variability (HRV) signals are extracted from ECG. It contains the relevant information of the cardiac movements. Congestive heart failure (CHF) is a cardiac disease in which heart is not able to pump sufficient blood to all the parts of the body. This study aims to diagnose the CHF accurately using HRV signals. We have used eigenvalue decomposition of Hankel matrix (EVDHM) method to decompose the HRV signals. The criteria to select the significant decomposed components are defined in this work. Thereafter, nine features corresponding to the five parameters: mean and standard deviation of the signal, mean frequency calculation using Fourier Bessel series expansion, k-nearest neighbour (kNN) entropy, and correntropy are evaluated from the decomposed components. The obtained features obtained are normalized with z-score normalisation method and then the student's *t*-test is used to evaluate the differentiation ability of the features. The ranked features based on *t*-values are then supplied as input to the least-squares support vector machine (LS-SVM) classifier with radial basis function (RBF) kernel for automated diagnosis of CHF HRV signals.

We have tested our method for three combinations of dataset. The combination with the best results obtained an accuracy of 98.50%, sensitivity of 97.80%, and specificity of 99.20% with HRV signals of the segment length of 500 samples and an accuracy of 98.83%, sensitivity of 99.23% and specificity of 98.33% for HRV signals corresponding to the segment length of 2000 samples. Our proposed method can aid the cardiac physicians in accurate diagnosis of CHF patients. Hence, it will help in providing timely treatment to CHF patients.

Contents

Acknowledgements	i
Abstract	iii
Contents	iv
List of Figures	vii
List of Tables	ix
Abbreviations	x
1 Introduction	1
1.1 Heart Structure and its Mechanism	1
1.2 Cardiovascular Diseases	3
1.3 Congestive Heart Failure: Causes, Symptoms and Diagnosis	4
1.4 Heart Rate Variability	6
1.5 Motivation	10
1.6 Thesis Organization	11
1.7 Summary	11

2	Eigenvalue Decomposition	13
2.1	Eigenvectors and Eigenvalues	13
2.2	EVD	14
2.3	EVD of Hankel matrix for the decomposition of multi-component signals	15
2.4	Selection of decomposition criteria in the present work	17
2.5	Summary	21
3	Database and Methodology	23
3.1	Databases used	24
3.2	EVDHM method	25
3.3	Computation of features	26
3.3.1	Computation of mean frequency using FB series expansion . .	29
3.3.2	kNN entropy measure	30
3.3.3	Correntropy	31
3.4	Feature selection and standardization	32
3.5	Classification	33
3.6	Summary	35
4	Results and Discussion	37
4.1	Results	37
4.1.1	HRV signals of length 500 samples	38
4.1.1.1	BD set 1	39
4.1.1.2	BD set 2	39
4.1.1.3	FD set	40
4.1.2	HRV signals of length 2000 samples	41
4.1.3	BD set 1	42
4.1.4	BD set 2	43

4.1.5	FD set	44
4.2	Discussion	45
4.3	Summary	50
5	Conclusion and Future Work	51
	Bibliography	53

List of Figures

1.1	ECG signal	7
1.2	HRV signal of normal subject.	8
1.3	HRV signal of CHF subject.	8
2.1	Considered HRV signal segment.	18
2.2	Signal constructed from the highest eigenvalue	19
2.3	Original signal and approximated signal with 10% STP criteria	19
2.4	Signal constructed from the second highest eigenvalue	20
2.5	Original signal and approximated signal with 1% STP criteria	20
2.6	Original signal and approximated signal as defined by the proposed method	21
3.1	Proposed system for the automated diagnosis of CHF.	24
3.2	Plot of (a) a normal HRV signal; (b) its decomposed 10 components using EVDHM method; (c) its LFC and HFC components.	27
3.3	Plot of (a) a CHF HRV signal; (b) its decomposed 10 components using EVDHM method; (c) its LFC and HFC components.	28
4.1	Accuracy versus kernel parameter for BD set 1, set 2, and FD set using 500 samples of HRV signals with LS-SVM classifier.	38
4.2	Accuracy versus number of features plot for BD set 1, set 2, and FD set using 500 samples of HRV signals with LS-SVM classifier.	39

4.3	Accuracy versus kernel parameters for BD set 1, set 2, and FD set using 2000 samples of HRV signals with LS-SVM classifier.	43
4.4	Accuracy versus number of features plot for BD set 1, set 2, and FD set using 2000 samples of HRV signals with LS-SVM classifier.	43

List of Tables

3.1	Details of HRV signals used from different databases.	25
4.1	Mean and SD values of ranked features with t-value for normal (MIT-BIH database) and CHF classes using 500 samples of HRV signals. . .	40
4.2	Mean and SD values of ranked features with t-value for normal (Fantasia database) and CHF classes using 500 samples of HRV signals. .	41
4.3	Mean and SD values of ranked features with t-value for normal (MIT-BIH NSR database and Fantasia database) and CHF classes using 500 samples of HRV signals.	42
4.4	Mean and SD values of ranked features with t-value for normal (MIT-BIH database) and CHF classes using 2000 samples of HRV signals. .	44
4.5	Mean and SD values of ranked features with t-value for normal (Fantasia database) and CHF classes using 2000 samples of HRV signals. .	45
4.6	Mean and SD values of ranked features with t-value for normal (MIT-BIH NSR database and Fantasia database) and CHF classes using 2000 samples of HRV signals	46
4.7	Summary of automated diagnosis of CHF using HRV signals.	49

Abbreviations

AV	Atrioventricular Valve
BD	Balanced Dataset
BIDMC	Beth Israel Deaconess Medical Center
BSA	Bispectral Analysis
CHF	Congestive Heart Failure
CAD	Coronary Artery Disease
CVD	Cardiovascular Disease
DFA	Detrended Fluctuation Analysis
DWT	Discrete Wavelet Transform
ECG	Electrocardiogram
EEG	Electroencephalogram
EF	Ejaculation Fraction
EMD	Empirical Mode Decomposition
EVD	Eigenvalue Decomposition
EVDHM	Eigenvalue Decomposition of Hankel Matrix
FAWT	Flexible Analytic Wavelet Transform
FB	Fourier Bessel
FD	Full Dataset
FN	False Negative
FP	False Positive
GDA	Generalised Discriminant Analysis
HF	Heart Failure

HFC	Highest Frequency Component
HRV	Heart Rate Variability
kNN	k-Nearest Neighbour
IMF	Intrinsic Mode Function
LFC	Lowest Frequency Component
LS-SVM	Least Square - Support Vector Machine
MF	Mean Frequency
MIT-BIH	Massachusetts Institute of Technology - Beth Israel Hospital
NSR	Normal Sinus Rhythm
RBF	Radial Basis Function
SD	Standard Deviation
STP	Significant Threshold Point
SVM	Support Vector Machine
TN	True Negative
TP	True Positive

Chapter 1

Introduction

For the proper functioning of the human body, the organs require oxygenated blood rich in nutrients. Circulating blood transports nutrients, oxygen and other necessary elements to and from the cells of the body [1]. The circulation of blood is studied under the circulatory system, also called cardiovascular system. Blood flows through the vessels of the circulatory system. Pumping activity of the heart regulates the blood flow through the vessels of the circulatory system. Disorders involving heart and blood vessels can lead to cardiovascular diseases [2]. A very common cardiovascular disease, in which the pumping action of the heart is affected is congestive heart failure (CHF). The structure of the heart and its mechanism is explained in next section.

1.1 Heart Structure and its Mechanism

Human heart has four chambers, left atria, right atria, left ventricles, and right ventricles [3]. Left atrium and ventricle are referred as left heart and the right atrium

and ventricle are together referred as right heart [4]. Left atrium is the smallest and the left ventricle is the largest among all the four chambers. The heart uses four valves to ensure blood flow in and out of the heart. Like the heart chambers, it has four valves, two semilunar valves and two atrioventricular (AV) valves [3].

Valve located between ventricle and atrium is AV valve. Mitral valve and Tricuspid valve are two AV valves that are present on the left and right side respectively, between the atrium and ventricle [3]. This valve opens when the pressure in the atrial side is greater than the pressure on the ventricular part. The valve closes again when ventricular pressure exceeds the atrial pressure. Aortic valve and Pulmonary valve are types of semilunar valves.

Aortic valve is between the aorta and left ventricle while pulmonary valve is between the pulmonary artery and the right ventricle [3, 4]. Aortic valve opens when the pressure in right or left ventricle exceeds pulmonary or aortic artery pressure.

Rhythm of the heart is determined by the sinoatrial node which is a cluster of pacemaking cells and it is located in the upper part of right atrium [2, 3]. From the systematic circulation, the heart receives the deoxygenated blood which enters the right atrium from body (through veins- superior and inferior venae cavae) and then passes to the right ventricle with the opening of tricuspid valve [2, 3, 4]. It is then pumped into the pulmonary circulation, in which pulmonary valve opens and the blood in right ventricle is pumped to the lungs through pulmonary artery. In lungs, oxygen is added to the blood and then it is passed to left atrium through pulmonary veins and then to left ventricles [4]. From left ventricles this oxygen rich blood is pumped to the rest part of the body through aorta. The sequence of receiving the deoxygenated blood in right atrium to the passage of oxygenated blood from right ventricle to body parts constitutes a cycle, called cardiac cycle [2]. This cycle continues without any disruption. The heart regulates the flow of blood

through blood vessels. Arteries and veins are two types of blood vessels, where veins are meant to carry the deoxygenated blood while arteries carry oxygen rich blood [2]. Pulmonary artery and pulmonary vein are exception to the defined properties of artery and vein. Pulmonary vein carries oxygenated blood from lungs to the left atrium and pulmonary artery carry deoxygenated blood from right ventricle to lungs. Any blockages in the blood vessel disturbs the circulation of blood and this may lead to disorders resulting in dysfunction of some body organs as it will not get proper supply of oxygen rich blood with proper nutrients. Some of these cardiac disorders are discussed in next section.

1.2 Cardiovascular Diseases

Disorders involving heart and blood vessels are called cardiovascular diseases (CVD) [5]. Many CVDs are related to the atherosclerosis. Under this condition, a substance, plaque develops in walls of arteries [6]. Its presence narrows the arteries, and it disturbs the flow of the blood across [6]. If the clotting of the blood takes place, blood flow may be stopped and cause heart attack. Some of the other important CVDs are coronary artery diseases (CAD), heart arrhythmias, heart valve problems, hypertensive heart disease, rheumatic heart disease, cardiomyopathy, congenital heart disease and CHF [7]. Arrhythmias is a condition which is related with abnormal rhythm of heart [8]. Heart valve problems are structural problems which arise when the heart valve does not open enough for the passage of blood [9]. All these disorders disturb the blood flow in the circulation system. CHF is a condition in which the pumping action of the blood is affected and its early diagnosis is required for medication to work effectively. CVD lead to more deaths in the world than any other disease [10] of which CHF forms one of the major parts.

1.3 Congestive Heart Failure: Causes, Symptoms and Diagnosis

If the pumping action of the heart gets affected, it would obstruct blood circulation and the flow of necessary nutrients to the body cells which will affect the normal functioning of the body. This complex and severe clinical syndrome are principally characterized by reduced myocardial contractility, diminished cardiac output, and hence not able to meet metabolic requirements of the body [11]. For the classification of CHF patients, measurement of ejection fraction (EF) is considered an important parameter [11]. The heart contracts and relaxes in each heartbeat. During contraction, the ventricle pumps out the blood and during relaxation, ventricles fill up. Even in the case of very strong contraction, ventricles are not able to pump out all the blood at once. The percentage of blood that a ventricle pumps out with each heartbeat is EF. It is usually measured only in the left ventricle because it is the major pumping chamber of heart that pumps the oxygenated blood to the other parts of the body. The CHF patients have reduced EF value [11].

Systolic and diastolic failures are two very common heart dysfunctions reported in most of the CHF patients [12]. The term systolic is related with contraction ability of the heart muscle. In systolic heart failure, heart becomes weak and enlarged which reduces the ability of heart to contract. In diastolic failure, the muscle becomes stiff and loses its relaxation ability [13]. Eventually blood and other fluids can back up inside lungs, liver and other parts of the body which deteriorates human health.

Some common symptoms are fatigue and shortness of breath that can limit the tolerance to exercise and cause fluid retention, which can further lead to splanchnic and pulmonary congestion [14]. Initial stage symptoms are fatigues, swelling in ankles and frequent urination. In the next stage of CHF, the condition of the

patient deteriorates and the symptoms are irregular heartbeat, shortness of breath and chest pain that radiates through the upper body [14].

Diagnosis of CHF patients is based on history, physical examination, electrocardiography (ECG) and echocardiography [15]. The symptoms may draw some medical attention but these symptoms are not specific to heart failure (HF), especially symptoms at the early stages, and therefore, may not discriminate between HF and other problems [16]. Many symptoms of the HF result from the sodium and fluid retention (e.g. peripheral oedema), and therefore these are not specific. They resolve quickly with the diuretic therapy. It is harder to detect more specific signs and hence, less reproducible. In the patients with chronic lung disease, obese individuals and in the elderly, it becomes difficult to interpret the signs and symptoms.

Medical history of patient is also very important. Persons without any relevant medical past that may have the potential to lead some kinds of cardiac damage are less likely to be the patient of HF [17], whereas those with the medical history that includes the certain features like myocardial infarction may increase the probability of being an HF patient.

The echocardiogram and ECG are another tests for suspected HF patients that are very useful. An echocardiogram captures the heart's image with the help of the sound waves and it is also referred as cardiac echo [18]. Ventricular diastolic and systolic function, thickness of the wall, functions of the valves and chamber volumes are immediately provided by the echocardiogram [19]. These information are very important in the diagnosis and appropriate treatment. The ECG presents the rhythm of the heart and the electrical activity.

It gives information about several cardiac disorders such as blockages in AV, sinoatrial disease, abnormal intraventricular conduction and its findings are considered very important which making decisions for the treatment [20].

In literature, there are numerous studies based on the ECG recordings which help in the identification of cardiac and non-cardiac diseases. Heart rate variability (HRV) signals that are extracted from ECG are also considered very important and have been widely studied for the diagnosis of cardiac disorders [21]. The study of HRV signals, its way of obtaining and its importance are discussed in the next section.

1.4 Heart Rate Variability

The HRV signals are widely used in as a clinical tool for the autonomic assessment and diagnosis of the CVD [22]. The HRV signals are obtained from ECG recording [21].

The ECG is a process in which electrodes are placed on the body parts and the electrical movements of heart is recorded for a certain period of time [23]. These electrodes are able to detect the small changes in the electrical activities on the skin that appear due to the depolarisation and repolarisation process that represent an electrophysiologic pattern of heart muscle during each heartbeat [23]. It is a cardiology test that is commonly performed for heart related problems. In biology, the process of depolarisation involves the changes within a cell, wherein the distribution of the electric charge in the cell varies that results in less negative charge in the cell. It is essential for the functioning of various cells, communication among them, and the overall organism's physiology [24]. After the phase of depolarisation that resulted in a positive value of the cell membrane, negative value resumes owing to change in membrane potential, it is referred as repolarisation [25].

In the conventional way, ECG is recorded by positioning the 10 electrodes on the chest's surface and the limbs of the patients [23]. The overall magnitude of the heart's electrical potential is then measured from 12 different angles and is recorded

over a period of time (usually 10 seconds). With this arrangement, in every cardiac cycle, all the moments are recorded that result from the electrical depolarisation and repolarisation of the heart [23]. A sample of recorded ECG signal is shown in Figure 1.1. The data points corresponding to this figure is taken from PhysioBank Massachusetts Institute of Technology - Beth Israel Hospital (MIT-BIH) normal sinus rhythm (NSR) database [27]. Vertical axis shows the amplitude of the voltages resulting due to depolarisation and repolarisation potential. This reading is taken in continuous time domain which is then sampled for the analysis purposes.

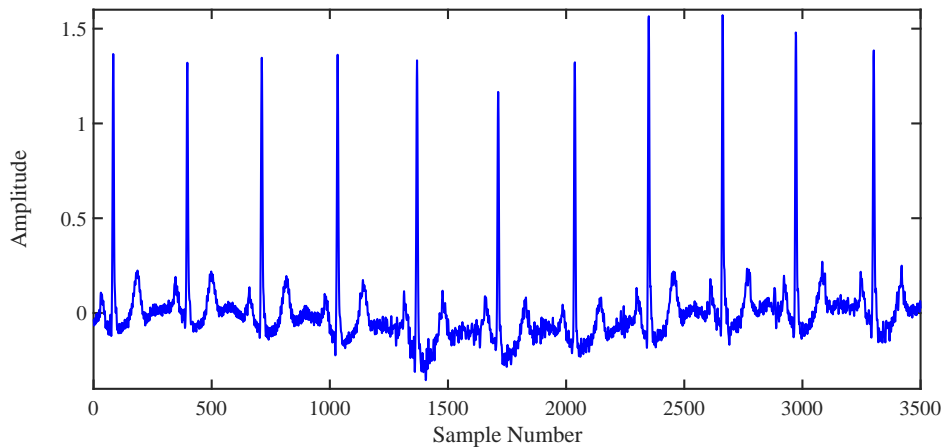


FIGURE 1.1: ECG signal

We can see for the Figure 1.1 that a pattern gets repeated. This pattern is categorised in few regions with the help of few points which are P, Q, R, S and T. A normal ECG recording consists of P-wave followed by QRS-complex and T-wave. P wave occurs due to left and right atrial depolarization whereas left and right ventricular depolarization causes QRS-complex [26]. T-wave corresponds to ventricular repolarization. R wave has the maximum amplitude [26] and it is considered very important because even in the case of noisy recorded data, because of its high amplitude its sample location can be distinguished easily. The plot of R-R interval against the number of samples forms the HRV signal [7].

Clinical studies of a wide spectrum of cardiac and non-cardiac ailments involve the analysis of HRV Signals [28]. Figures 1.2 and 1.3 show HRV signals of normal and CHF subjects. Data points of Figures 1.2 and 1.3 are obtained from Physiobank MIT-BIH NSR database [27] and Beth Israel Deaconess Medical Center (BIDMC) database [27, 29], respectively. More details of these database is given in Chapter 3.

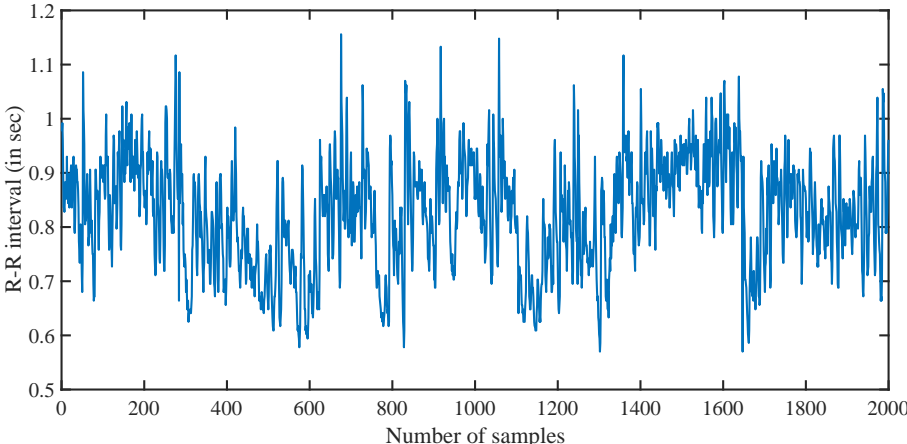


FIGURE 1.2: HRV signal of normal subject.

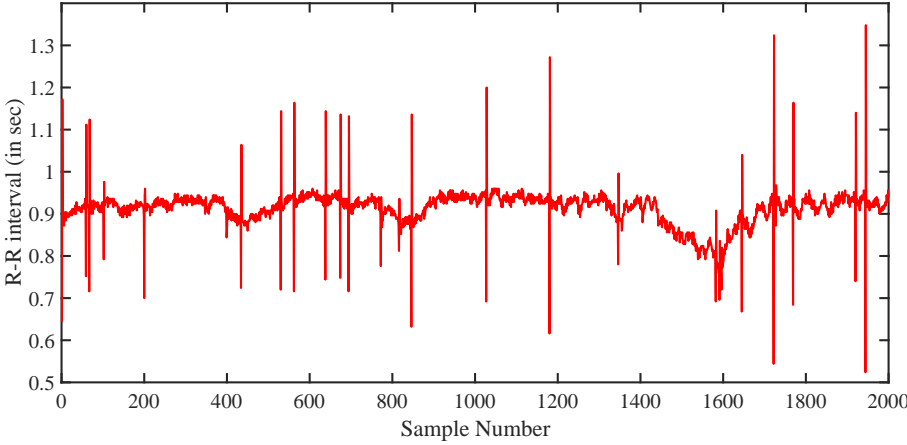


FIGURE 1.3: HRV signal of CHF subject.

The unique information present in the pattern of HRV signals helps in the identification of disease, but it is tedious to detect visually. Moreover, diagnosis by visual inspection may be subjective in identification of heart disease. Therefore, various

automated classification methods using HRV signals have been proposed in the literature. CAD is automatically diagnosed with the help of HRV signals in [30, 31, 32]. Entropy based features with flexible analytic wavelet transform (FAWT) are used for CAD diagnosis from HRV signals [32]. The features extracted from the intrinsic mode functions (IMFs) for CAD analysis from HRV signals have been studied in [33]. Diabetes is automatically diagnosed using HRV signals [34, 35]. A study based on discrete wavelet transform (DWT) with approximate entropy and sample entropy has been performed for diabetes prognosis using HRV signals [34]. The Fourier-Bessel (FB) series expansion based features are used for the diagnosis of diabetes [36]. Hypertension patients are also investigated using HRV signals in [37].

The statistical analysis of HRV signals performed in [38] concluded that the reduction in standard deviation of R-R interval is an indicator of HF. Power in very low frequency range of HRV signal is a predictor of CHF disease [39]. The nonlinear methods used on HRV signals for the classification of normal and CHF subjects include Poincare plot [40] and detrended fluctuation analysis (DFA) [41]. A long-term HRV signal has been employed for CHF detection using a method based on optimal classification and regression tree [42]. A correlation between nonlinearity of HRV signals and different risk levels of CHF patients are analysed in [43]. The generalised discriminant analysis (GDA) has been studied for long-term HRV signals, where non-linear features have shown better results than the linear features [44]. Recently, authors have extracted various entropy based features from IMFs in [16] such as accumulated fuzzy and permutation entropies for CHF diagnosis with HRV as base signal [32].

1.5 Motivation

The CHF results in reduced myocardial contractility, less cardiac output, and consequently metabolic requirements of the body is not fulfilled. The consequences of these changes are breathlessness, severe fatigue, and ultimately death [45]. Therefore, the diagnosis of HF at an early stage is very important. Various studies based on HRV discussed in previous section highlight the facts that analysis of HRV signals provides useful information about the CHF state.

Although these techniques are very informative and useful for the diagnosis of CHF patients but the reliability and reproducibility of these techniques are still problematic in this field. For the noninvasive treatment, better and more refined techniques are still required.

Therefore, this work emphasizes on the extraction of features using eigenvalue decomposition of hankel matrix (EVDHM) [46] which is able to capture the fine variations of the HRV signals that helps in the identification of CHF. The EVDHM has been used for speech signal analysis in [47]. The fundamental frequency of speech signal has been obtained from the EVDHM method in [48]. A new method for the time-frequency representation, that is based on EVDHM is given in [49]. This paper presents an application of EVDHM method for the analysis and classification of HRV signals for diagnosis of CHF.

1.6 Thesis Organization

Rest of the thesis work are structured as follows: In Chapter 2, the eigenvalue decomposition (EVD) process is described, where the signal decomposition is discussed. Feature extraction and classification techniques are presented under proposed methodology section discussed in Chapter 3. Results are presented and discussed in Chapter 4. Chapter 5 provides the conclusion and directions for future works.

1.7 Summary

The CHF is a cardiovascular disorder wherein the pumping action of the heart is affected and the blood circulation process is disturbed. Clinicians physically examine the patients, refer their medical history and observe ECG and echocardiography readings to diagnose the CHF patients. Echocardiography produces images with the help of echo waves which is helpful in predicting the cardiac disorders. ECG is the another important noninvasive test in which hearts's electrical activity is recorded. HRV signals are extracted from the ECG and it is widely used to study the cardiac behaviour. In literature, HRV signals of CHF patients have been studied but a reliable technique for the identification of CHF patients is still needed. In this work, we have studied the HRV signals of normal and CHF subjects and proposed a technique for the identification of CHF patients.

Chapter 2

Eigenvalue Decomposition

The first part of our proposed methodology is the decomposition of the HRV signals which involves the EVD technique that makes use of eigenvalues and eigenvectors which are special classes of scalars and vectors. In this chapter, we will explain EVD, decomposition of multicomponent signals using EVD of Hankel matrix, and selection of decomposition criteria.

2.1 Eigenvectors and Eigenvalues

The eigenvalues and eigenvectors are useful in many applications such as image segmentation [50], data transformation and reduction [51], ranking [52], etc. Mathematically it is explained below.

Let x be vector in a vector space X and T is a linear operator that operates on vector x so that it satisfies the following relation [53, 54]:

$$T(x) = \lambda x \tag{2.1}$$

Here, x is the eigenvector of the linear operator T . The transformation T which is applied on x scales the vector x with a factor λ .

If the linear operator is given by a matrix A , then, the above expression can be written as follows: then,

$$Ax = \lambda x \tag{2.2}$$

where, A is the system matrix, x is the eigenvector of matrix A and λ is the eigenvalue [53, 54].

2.2 EVD

In linear algebra, with the help of EVD, we decompose a matrix in terms of eigenvectors and eigenvalues .

For a matrix A , the EVD can be expressed as follows [53, 54, 55]:

$$A = V\Lambda V' \tag{2.3}$$

here, the columns of V contains the eigenvectors of the matrix A and the Λ is the diagonal matrix that contains all the eigenvalues in its diagonal.

2.3 EVD of Hankel matrix for the decomposition of multi-component signals

A multi-component non-stationary signal $x[l]$ of length $2L - 1$ forms a Hankel matrix [56], H_L^x , which is represented as follows [46]:

$$H_L^x = \begin{bmatrix} x[0] & x[1] & \cdot & \cdot & x[L-1] \\ x[1] & x[2] & \cdot & \cdot & x[L] \\ \cdot & \cdot & \cdot & \cdot & \cdot \\ \cdot & \cdot & \cdot & \cdot & \cdot \\ x[L-1] & x[L] & \cdot & \cdot & x[2L-2] \end{bmatrix} \quad (2.4)$$

The size of H_L^x , $L \times L$ is specified in the range $L \gg F_s/\delta x$, where F_s and δx represent the sampling frequency and least frequency separation between components, respectively.

The computed eigenvalue matrix Λ_x and the real eigenvector matrix, V_x of H_L^x , represent a relation [55] as follows:

$$H_L^x = V_x \Lambda_x V_x' \quad (2.5)$$

The eigenvalue matrix Λ_x have L eigenvalues out of which $\frac{L}{2}$ eigenvalues are positive values and rest are negative values. The eigenvalues of high magnitude are useful for the signal decomposition. The significant eigenvalues of Λ_x are considered with the significant threshold point (STP) criteria [46, 49] according to which the eigenvalues that come under the range of 10% of magnitude of maximum eigenvalue are considered as significant eigenvalues.

Each significant eigenvalue pair is used to extract the component. Therefore, new eigenvalue matrix based on the s^{th} eigenvalue pair is formed as follows:

$$\check{\Lambda}_x^s = \begin{bmatrix} 0 & 0 & \dots & 0 & 0 \\ 0 & \lambda_{x_s} & \dots & 0 & 0 \\ \cdot & \cdot & \dots & \cdot & \cdot \\ \cdot & \cdot & \dots & \cdot & \cdot \\ 0 & 0 & \dots & \lambda_{x_{P-s+1}} & 0 \\ 0 & 0 & \dots & 0 & 0 \end{bmatrix} \quad (2.6)$$

The new eigenvalue matrix $\check{\Lambda}_x^s$ replaces Λ_x in (2.5) and results in a new reconstruction matrix for the s^{th} component, which is represented as:

$$\check{H}_L^{x_s} = V_x \check{\Lambda}_x^s V_x' \quad (2.7)$$

The mean of anti-diagonal elements of $\check{H}_L^{x_s}$ provides the samples of the s^{th} component.

The construction $L \times L$ Hankel matrix requires a signal length of $2L-1$ samples, which is an odd number. In this work, we have used HRV signals of the lengths 2000 samples and 500 samples for the analysis. Therefore, for the decomposition purpose, the EVDHM method takes 1999 samples and 499 samples, respectively for both the signal lengths.

2.4 Selection of decomposition criteria in the present work

When we processed the HRV signals with the method mentioned in section 2.3, we came across the fact that with the given 10% STP criteria [46], the obtained components failed to approximate the original signal. Thus, we lowered the threshold level to include more components which when added, shall effectively reproduce the original signal. We varied the STP criteria from 10% to 1%, but still, the decomposed components did not add up to approximate the original signal. It failed to capture the variations present in the signal. To demonstrate this, we take an HRV signal of normal subject with a segment length of 2000 samples from MIH-BIH NSR database, the details of the dataset used in our work is explained in chapter 3.

The HRV signal which is to be decomposed is shown in Figure 2.1. We first create a Hankel matrix from this signal and decompose the matrix as per the method described above. As the signal is of 2000 samples, the EVDHM considers 1999 samples for processing. Hence, the order of Hankel matrix will be 1000×1000 . After the first iteration, we obtained 1000 eigenvalues of which the highest eigenvalue obtained was 592.8714 and the second highest value was 20.1355. Now, with the 10% STP criteria, the 10 percent of 592.8714 is calculated which comes to be 59.8714 and only those components get selected which have an eigenvalue greater or equal to 59.8714. As the second highest eigenvalue is only 20.1355, this gives only one significant component. As per the components merging criteria [46], the significant components when added shall always approximate to the original signal. Figure 2.2 shows the signal corresponding to the highest eigenvalue and as this is the only significant component obtained with 10% STP criteria, this is the approximated original signal. This approximated signal is plotted together the original signal in Figure 2.3. From this figure, it can be visualized that the approximated signal is

not able to trace the variations present in the original signal. Therefore, in the next step we will vary the standard STP criteria [46] and decrease the threshold limit so that we can get more components. We decreased the STP percentage criteria from 10% to 1% with a step size of 1%. Here, we will show the results that we obtained with 1% STP criteria, which could collect the maximum components compared to other higher levels of threshold condition. When applied the 1% STP criteria on the same HRV signal, only two eigenvalues fulfilled this criteria, one with the highest eigenvalue 592.8714 and the other with eigenvalue 20.1355. We have already seen the signal corresponding to the highest eigenvalue in Figure 2.2 . Signal corresponding to another significant eigenvalue is shown in the Figure 2.4 . Now, these two significant components when added shall reproduce the signal. Approximated signal with 1% STP condition and the original signal are shown in Figure 2.5 . It can be perceived from the Figure 2.3 and Figure 2.5 that the second condition is somewhat better than the first in the process of reproducing the original signal, but still, the reproduced signal is not able to approximate the original well.

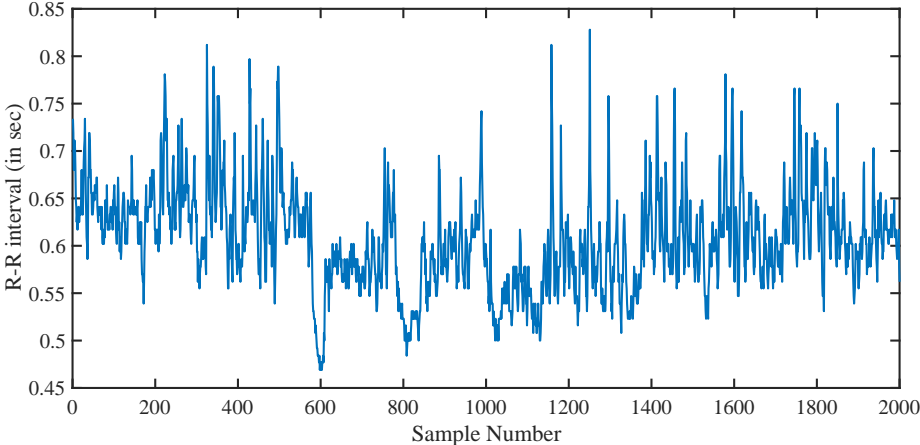


FIGURE 2.1: Considered HRV signal segment.

If we are able to get more significant components so that the relevant information of the signal is not lost and approximated signal can well capture the variations of the original signal, we can proceed further and would be able to extract the features

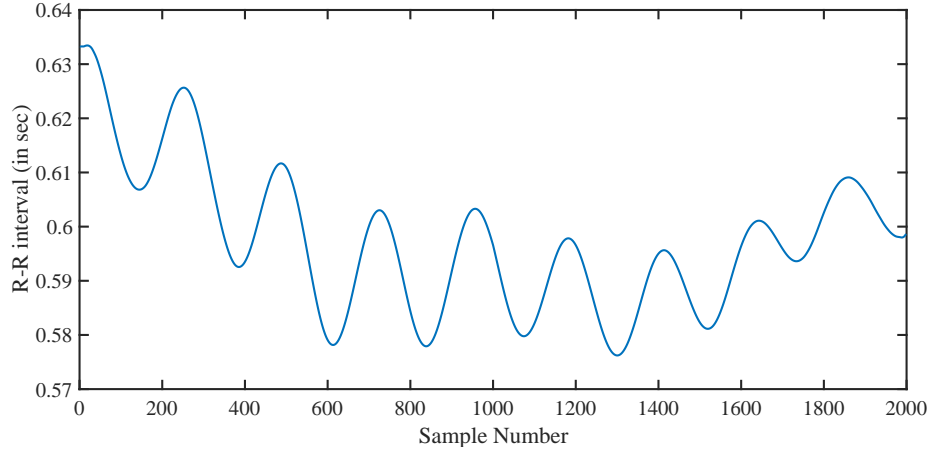


FIGURE 2.2: Signal constructed from the highest eigenvalue

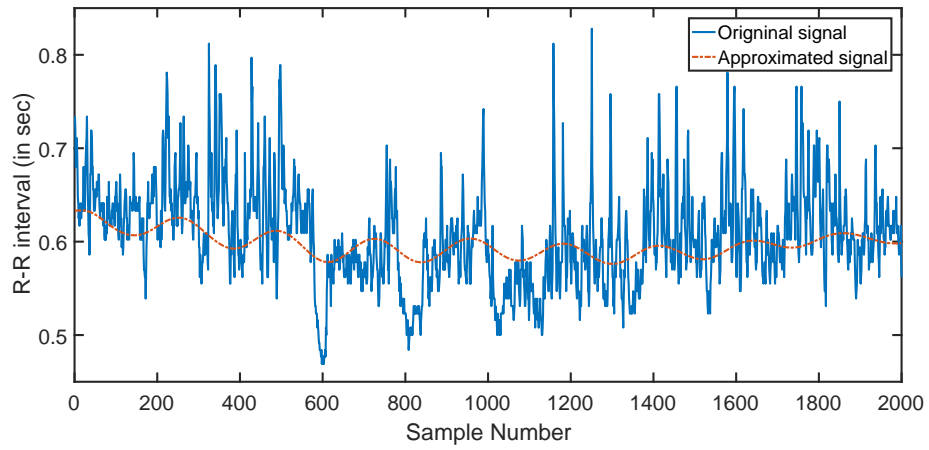


FIGURE 2.3: Original signal and approximated signal with 10% STP criteria

that can lead to better classification accuracy. With an aim to include the relevant information present in the quick variations of HRV signal, we have proposed the selection of the first 10 significant decomposed components which would keep the relevant information present in the signal. Proceeding with the same HRV signal, we have taken 10 significant components and tried to reconstruct the signal. The approximated signal is better than what we obtained in the STP conditioned cases mentioned above and it is shown in Figure 2.6 . From this figure, we can observe that this approximated signal is able to capture the variations of HRV signal on a larger

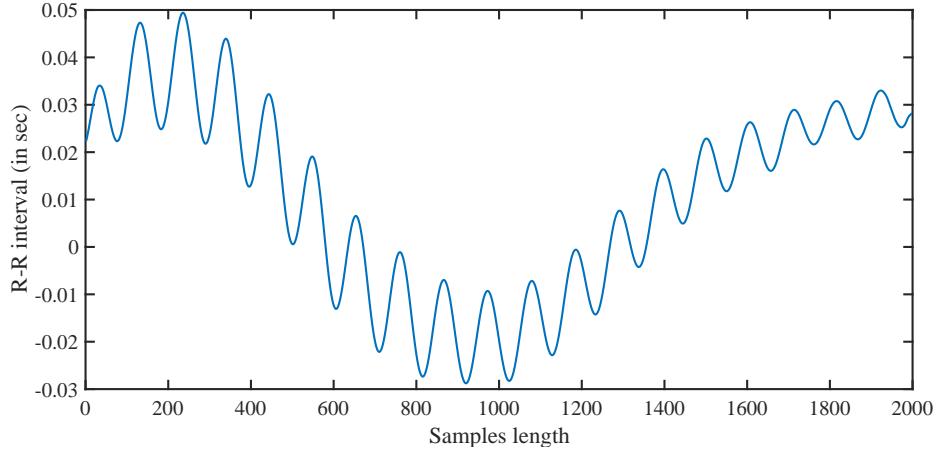


FIGURE 2.4: Signal constructed from the second highest eigenvalue

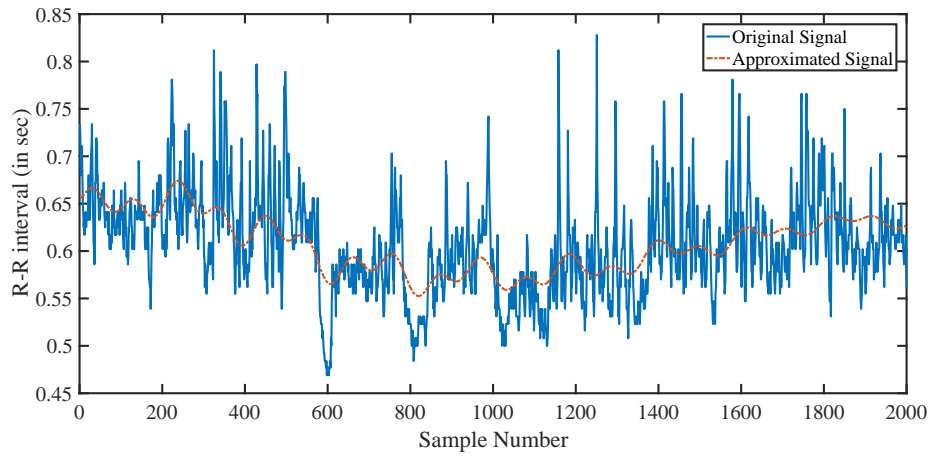


FIGURE 2.5: Original signal and approximated signal with 1% STP criteria

scale as compared with the previous ones obtained using STP criteria. Though, the STP criteria works well for other signals, like speech signals [47] but here, in the case of the HRV signals, it is not able to reproduce the original signal well. Thus, we have proceeded with the proposed technique to decompose the HRV signals. The next steps are discussed in the methodology section in Chapter 3.

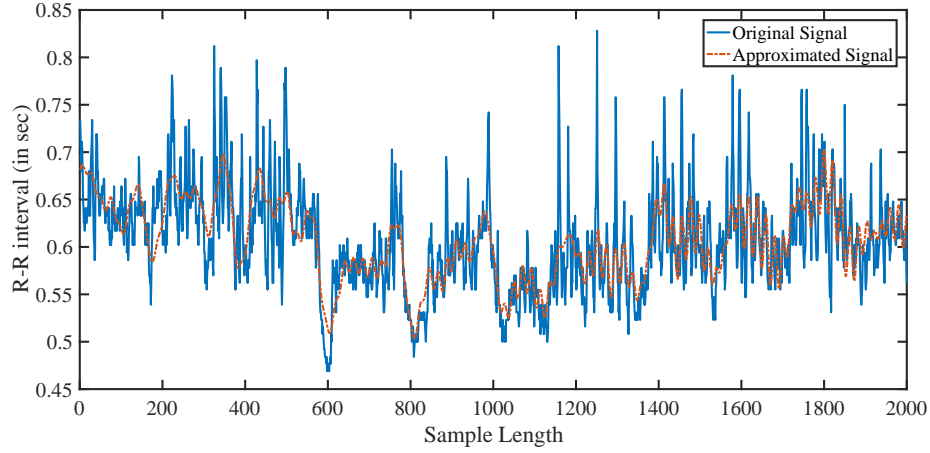


FIGURE 2.6: Original signal and approximated signal as defined by the proposed method

2.5 Summary

If a linear transformation of input vector results in a output with a scalar multiple of input vector, then the scaled value is the eigenvalue and the input vector is the eigenvector corresponding to linear operator. This remains the basis of the EVD process. HRV signal is first processed with EVDHM method. The STP criteria explained in [46] is not found to be suitable for our work which is demonstrated above with the help of an HRV signal that we have used in this work. We have used the component selection criteria based on the significant eigenvalues. Eigenvalues are then ranked by its absolute value from highest to lowest. Components corresponding to first ten ranked eigenvalues are selected as significant components.

Chapter 3

Database and Methodology

In this chapter, we present the methodology that have been used to design the automated technique for the identification of CHF patients. This chapter also contains the information of the databases that have been used for processing. The steps carried out in the proposed method are shown in the Figure 3.1. At first the HRV signals of normal and CHF subjects are collected. These signals are decomposed using EVDHM technique, an overview of which has been given in Chapter 2. Once the decomposed components are available, the next step is the feature extraction. In this step, we extract certain features of the highest frequency component (HFC) and lowest frequency component (LFC) of the HRV signal. Next step is the feature ranking which ranks the features according to their class discrimination ability. The ranked features are then fed to classifier which trains itself with the some of the feature vector of all classes. Here, we have two classes namely, normal and CHF. After the training, the classifier performs the testing part in order to identify the true classes of the rest of the features which were not used in the training part.

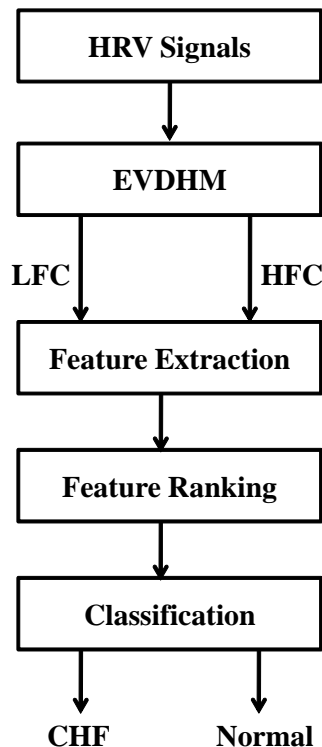


FIGURE 3.1: Proposed system for the automated diagnosis of CHF.

3.1 Databases used

The databases used in this work were obtained from PhysioBank MIT-BIH NSR [27], BIDMC CHF dataset [27, 29] and Fantasia [57, 27]. The detailed information of these databases is presented in Table 3.1. The HRV signals of 15 (11 males and 4 females) CHF patients were obtained from BIDMC CHF database with a recording length of 20 hours per person. The normal signals have been obtained from the 58 (20 old, 20 young, 5 males and 13 females) normal subjects which have been taken from Fantasia and MIT-BIH NSR databases. Recording length for MIT-BIH NSR was 24 hours. Fantasia database has the recording length of two hours.

Subjects in Fantasia stayed in resting posture in the sinus rhythm while they watched the movie 'Fantasia' (Disney, year-1940) to maintain wakefulness. A total 58 HRV

TABLE 3.1: Details of HRV signals used from different databases.

Information		Class 1 (CHF)	Class 2 (Normal)	
Database		BIDMC	MIT-BIH NSR	Fantasia
Patient details		11 males (age 22 years to 71 years)	5 males (age 26 years to 45 years)	20 young (age 21 years to 34 years)
		4 females (age 54 years to 63 years)	13 females (age 20 years to 50 years)	20 elderly (age 68 years to 85 years)
500 samples	BD 1 set	500 segments	500 segments	-
	BD 2 set	500 segments	-	500 segments
	FD set	3212 segments	3420 segments	500 segments
2000 samples	BD 1 set	125 segments	125 segments	-
	BD 2 set	125 segments	-	125 segments
	FD set	803 segments	855 segments	125 segments

recordings of normal subjects and 15 HRV signals of CHF patients are considered in this study. The HRV signals are segmented into 500 samples and 2000 samples for this study. Two categories of dataset, namely balanced dataset (BD set) and full dataset (FD set) are taken for both types of segment size corresponding to of sample lengths 500 and 2000 of HRV signals. The balanced sets are further categorized into two sub-categories namely, balanced set 1 (BD set 1) and balanced set 2 (BD set 2). The details of all sets are given in Table 3.1.

3.2 EVDHM method

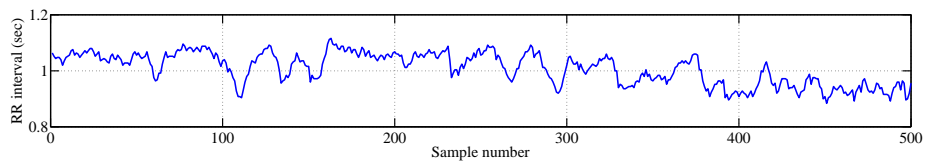
The HRV signal is first decomposed with the EVDHM method. In this, we first form a Hankel matrix from the HRV signal and decompose as per the steps discussed in Chapter 2. Now, instead of going for iterative process of decomposing again and again, we just extract ten significant components corresponding to the highest

eigenvalue pairs of Hankel matrix. All these ten components are arranged in the increasing order of center frequency of each component. Then, the components corresponding to the lowest and the highest frequency are selected for the next step, i.e, feature extraction. A normal HRV signal is shown in Fig. 3.2(a) and its 10 decomposed components are shown in Figure 3.2(b). The LFC and HFC obtained from the signal shown in Figure 3.2(a) are depicted in Figure 3.2(c). Similarly, the decomposed components of a CHF HRV signal shown in Figure 3.3(a) are presented in Figure 3.3(b). The obtained LFC and HFC for this CHF HRV signal are shown in Figure 3.3(c). In the next section, the features which have been extracted are explained.

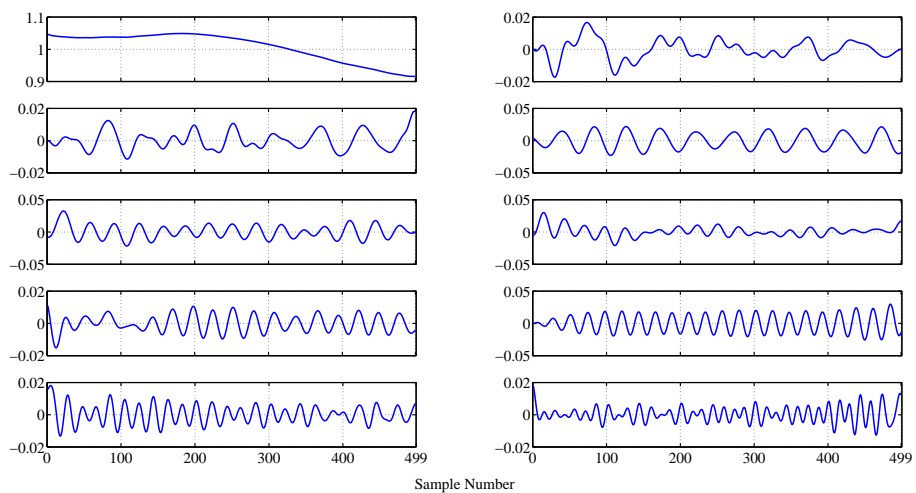
3.3 Computation of features

Feature extraction process helps to represent characteristics of the signals in unique way. The extracted features are very useful for the classification of biomedical signals of normal and abnormal classes.

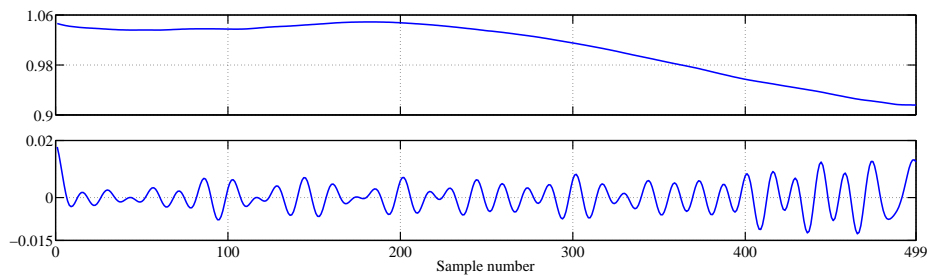
It has been observed that both linear and the non-linear features are useful for the classification purpose of the normal and CHF HRV signals [44, 58]. In this work, a total of nine features corresponding to five parameters namely mean and standard deviation (SD) of the signal (mt and st) [59], mean frequency (MF) of the signal using Fourier Bessel (FB) expansion, k-nearest neighbourhood (kNN) entropy measure [60] and correntropy [61] are extracted. The MF using FB series expansion, kNN entropy and correntropy are discussed in the next section.



(a)

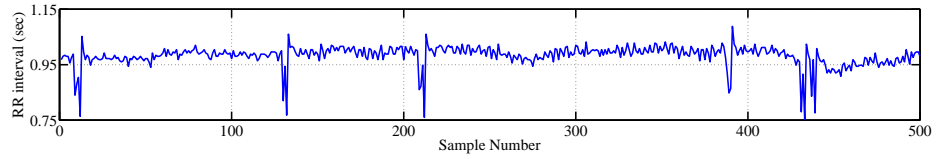


(b)

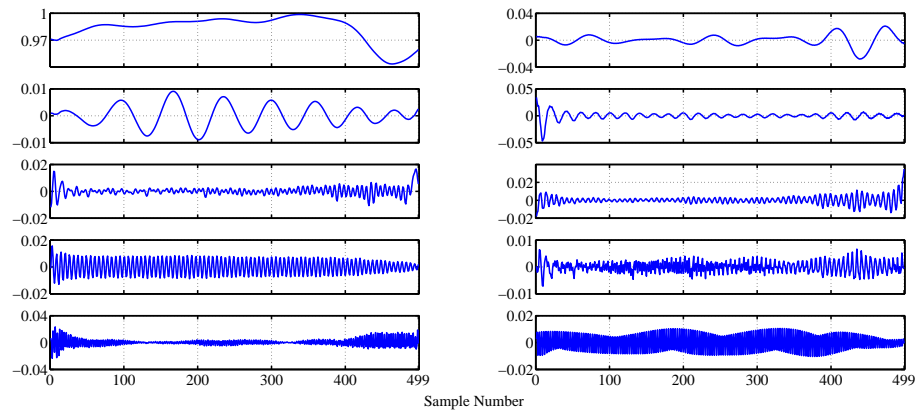


(c)

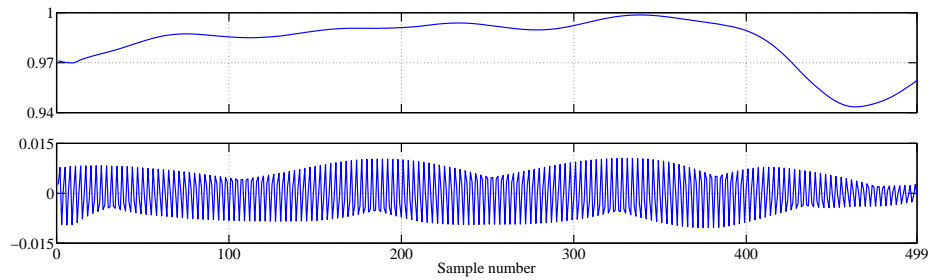
FIGURE 3.2: Plot of (a) a normal HRV signal; (b) its decomposed 10 components using EVDHM method; (c) its LFC and HFC components.



(a)



(b)



(c)

FIGURE 3.3: Plot of (a) a CHF HRV signal; (b) its decomposed 10 components using EVDHM method; (c) its LFC and HFC components.

3.3.1 Computation of mean frequency using FB series expansion

Aperiodic and decaying nature of Bessel functions make them suitable to represent nonstationary signals using FB series expansion. Analysis of multicomponent signals using FB series expansion has been studied in [62, 63]. Consider a signal $x(t)$ over an interval $(0, b)$, then its zero-order FB series expansion is given as follows [64]

$$x(t) = \sum_{n=1}^P C_n J_0\left(\frac{z_n}{b}t\right) \quad (3.1)$$

where, z_n are the roots of $J_0(z) = 0$ such that $z_m > z_n$ for $m > n$ and $J_0\left(\frac{z_n}{b}t\right)$ is the Bessel function of zero-order.

In the interval, $0 \leq t \leq b$, the Bessel functions form an orthogonal set with respect to t , which can be given as [64]

$$\int_0^a t J_0\left(\frac{z_n}{b}t\right) J_0\left(\frac{z_m}{b}t\right) dt = 0 \quad (3.2)$$

The FB coefficients C_n are calculated as follows [64]:

$$C_n = \frac{2 \int_0^b tx(t) J_0\left(\frac{z_n}{b}t\right) dt}{b^2 [J_1(z_n)]^2} \quad (3.3)$$

where, $J_1(n)$ is Bessel function of first-order.

Thus the mean frequency can be computed as follows [65]:

$$f_{\text{mean}} = \frac{\sum_{n=1}^Q f_n E_n}{\sum_{n=1}^Q E_n} \quad (3.4)$$

where,

$$E_n = c_n^2 \frac{b^2}{2} [J_1(z_n)]^2 \quad (3.5)$$

Here, E_n is the energy at order n .

The FB expansion has been studied in different areas, such as, analysis of speech signal using FB expansion in [66], analysis of center of pressure signals [65], and analysis of Electrocardiogram (EEG) signals [67, 68].

3.3.2 kNN entropy measure

The kNN density estimators have been proposed in [69]. The kNN algorithm is used for both regression and classification purposes [70]. The kNN entropy is suitable for the analysis of HRV signals due to its nonlinear nature.

The kNN entropy of a variable x is estimated by the following expression [60, 71]

$$H_k = \psi(n) - \psi(k) + \log(c_d) + \frac{d}{n} \sum_{i=1}^n \log(p_i^k) \quad (3.6)$$

Here, n is the number of total samples that form the signal and d represents the dimension of x and p_i^k measures the distance between the i^{th} sample of the signal and its k nearest neighbors. The $\psi(y)$ denotes a digamma function which is given by following expression:

$$\psi(y) = \frac{1}{\Gamma_y} \frac{d\Gamma_y}{dy} \quad (3.7)$$

The c_d measures volume of the d -dimensional unit ball. The c_d is expressed as follows:

$$c_d = \frac{\pi^{\frac{d}{2}}}{\Gamma(1 + \frac{d}{2})} \quad (3.8)$$

In this work, dimension d is taken as 1.

The systematic metabolic disturbances in the patho-physiological states are computed using kNN entropy [71]. The kNN entropy is recently studied for CAD diagnosis in [32].

3.3.3 Correntropy

The correntropy is a nonlinear similarity measure between two random variables. The correlation between two signals can also be measured using correntropy [61, 72]. The correntropy of two signals Y_a and Y_b can be expressed as follows:

$$\text{Corr}(Y_a, Y_b) = E [k(Y_a - Y_b)] \quad (3.9)$$

where k is a symmetric, positive definite kernel function [73] and E is the expectation operator.

On considering two signals Y_a and Y_b which have samples $[y_{a_1}, \dots, y_{a_n}]$ and $[y_{b_1}, \dots, y_{b_n}]$, respectively. The correntropy, $\text{Corr}_{n,\sigma}(Y_a, Y_b)$ between Y_a and Y_b can be estimated as [61]:

$$\text{Corr}_{n,\sigma}(Y_a, Y_b) = \frac{1}{n} \sum_{i=1}^n K_{\sigma}(y_{a_i} - y_{b_i}) \quad (3.10)$$

In this work, kernel k is Gaussian kernel and therefore the correntropy has been calculated as follows [61]:

$$\text{Corr}_{n,\sigma}(Y_a, Y_b) = \frac{1}{n} \sum_{i=1}^n \exp\left(\frac{-\|y_{a_i} - y_{b_i}\|^2}{\sigma^2}\right) \quad (3.11)$$

The kernel parameter, σ is taken 1. The correntropy has been used as a cost function in linear adaptive filters [74]. It has also been studied for the nonlinear similarity measurement for the multichannel signals [75]. The CAD diagnosis using HRV signals [31] and focal EEG signal detection with FAWT in [76] also use correntropy based features. It has also been used in diagnosis of glaucoma from fundus images [77]. The study presented in [78] has used regularised correntropy for robust feature selection for the classification of breast cancer. The correntropy based matched filter for the classification in side-scan sonar imagery has been presented in [79]. The correntropy between LFC and HFC is evaluated in the proposed methodology.

3.4 Feature selection and standardization

Feature selection process helps to minimize computation time and may improve the performance of classification [80]. The student's t -test is performed to obtain the highly distinguishable features [34, 77, 81]. The t -test contains normal distribution property between feature sets to distinguish different classes. Features ranking is done based on the t -value as high t -value discriminates more. Therefore, higher t -value based features are used for performance evaluation process. Further, feature standardization is performed to normalise the features. It is operated with unit

standard deviation and zero mean, which is known as z-score normalization [82]. Mean value of data is subtracted from the data and thereafter, resultant is divided by the standard deviation of data. The normalized data \hat{z} can be characterized as [83]:

$$\hat{z} = \frac{z - \bar{z}}{\tilde{z}} \quad (3.12)$$

where, \tilde{z} represents the standard deviation and \bar{z} represents the mean of data z .

3.5 Classification

In this work, support vector machine (SVM) classifier is used for classification of the HRV signals corresponding to normal and CHF subjects. The SVM is a supervised machine learning method in which the classification is achieved with the help of input output mapping functions that is generated from a set of labeled training data [84]. Classifier model based on SVM method presents a set of data points in the feature space, which are mapped so that the data points of different classes are separated as far as possible. The new data is also mapped into the same space and obtained boundaries during training phase are used for separating the classes.

For the classification purpose, input data is presented in high dimensional space with the help of the kernel functions and the hyperplanes with the maximum margins are created so that the classes are better distinguished. Here, input data is presented into high dimensional space and the hyperplanes with maximum margins are created so that the classes are better distinguished.

The LS-SVM is a least square version of the SVM and it finds many applications in

real-world problems, such as, image processing [85], text categorization [86], character recognition [87], and bioinformatics [88]. It is widely used in biomedical applications such as seizure classification [89, 90, 91, 92, 93], diagnosis of cancer disease [94], diabetes diagnosis [34, 36], and CAD diagnosis [31, 32, 95, 96, 97].

Mathematically, the LS-SVM can be expressed as follows [84]:

$$y(p) = \text{sign} \left\{ \sum_{n=1}^N y_n \alpha_n K(p, p_n) + b \right\} \quad (3.13)$$

Here, b represents the bias term, α_n is the Lagrange multiplier, y_n denotes the target vector, p_n denotes n^{th} input vector of d -dimension, N is the number of input and output pairs that is used for training and K represents the kernel function that transforms input vector into higher dimensional space. In this work, radial basis function (RBF) kernel is used .

Mathematically, RBF kernel [98, 100] can be expressed as follows:

$$K(p, p_n) = \exp \left(\frac{-\|p - p_n\|^2}{\sigma^2} \right) \quad (3.14)$$

Three major performance evaluation parameters of LS-SVM classifier are accuracy denoted by Acc , specificity denoted by Spe and sensitivity denoted by Sen [101]. The Acc measures the proportion of correctly classified data out of total samples. The Sen measures the proportion of CHF patient's HRV signals that are distinguished correctly and the measure of the proportion of healthy person's HRV signals that are correctly identified is Spe .

If true positive (TP) represents the number of patient's HRV signals that are truly classified, true negative (TN) represents the number of healthy person's HRV signals that are truly classified and false positive (FP) presents the number of healthy person's HRV signals that are incorrectly classified as patient's data and false negative (FN) evaluates the number of CHF patient's HRV signals that are incorrectly classified as healthy persons data, then Sen, Spe, and Acc are expressed as follows [100]:

$$\text{Sen} = \frac{TP}{FN + TP} \times 100\% \quad (3.15)$$

$$\text{Spe} = \frac{TN}{TN + FP} \times 100\% \quad (3.16)$$

$$\text{Acc} = \frac{TN + TP}{FP + FN + TP + TN} \times 100\% \quad (3.17)$$

The ten-fold cross validation method has been explored with the LS-SVM classifier to ensure the robustness of the method [99]

3.6 Summary

Database of the HRV signals used in this work are publicly accessible database. Analysis and classification of the signals are done in two categories with two different sizes, one with a size of length of 2000 samples and the another with 500 samples. For both categories of sample size, three sets are formed, namely BD 1 set, BD 2 set and FD set. The HRV signals are then decomposed using EVDHM method and

the significant ten decomposed components are extracted and then arranged in the order of their centre frequency. Out of these ten components, only LFC and HFC components are considered for the next step. Next step is the feature extraction. Features corresponding to the mean and SD of the signal, mean frequency using FB expansion, kNN entropy, and correntropy are computed. With the help of these five parameters, a total of nine features are computed. These computed features are ranked with the t -test method which uses z-score normalisation. The ranked features are then supplied as an input to the LS-SVM classifier with RBF kernel. A ten fold cross-validation method in the LS-SVM classification process has been used. Finally, we evaluate the classifier's performance in terms of the Acc, Spe and Sen.

Chapter 4

Results and Discussion

We have processed the HRV signals as per the methodology described in Chapter 3. Before starting the processing part, we have categorised the dataset into two parts on the basis of segment length. Segments with size of 500 samples are processed in one part and the segments with the size of 2000 samples are processed in the other part. This is further divided in the two balanced and one unbalanced set as described in Chapter 3. The results obtained after processing HRV signals are discussed below.

4.1 Results

The EVDHM method is applied to each HRV signal to extract ten components based on dominant eigenvalue pairs in one iteration. The LFC and HFC are obtained from the decomposed components. Thereafter, features corresponding to five parameters are measured from the these components. The mean of LFC (mt_l), SD of LFC (st_l), mean of HFC (mt_h), SD of HFC (st_h), mean frequency of LFC (mf_l), mean frequency

of HFC (mf_h), kNN of LFC (kNN_l), kNN of HFC (kNN_h), and correntropy between LFC and HFC (Corr) are measured. Therefore, total 9 features are computed. Results for 500 and 2000 samples HRV signal are explained in next sections.

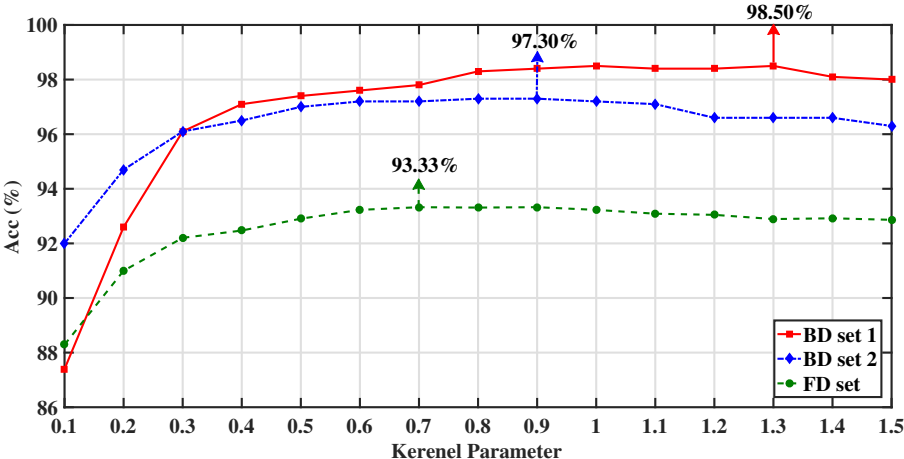


FIGURE 4.1: Accuracy versus kernel parameter for BD set 1, set 2, and FD set using 500 samples of HRV signals with LS-SVM classifier.

4.1.1 HRV signals of length 500 samples

In this section, we have worked on dataset with segment length of 500 samples. The 3920 segments belonging to 58 normal subjects and 3212 segments from 15 CHF subjects are considered.

BD set 1 and BD set 2 consist of 500 segments from both the classes. BD set 1 comprises of 500 segments of normal class (MIT-BIH NSR database) and 500 segments from CHF class (BIDMC database). BD set 2 contains 500 segments of normal class from Fantasia database and 500 segments from CHF class (BIDMC database). The FD set consists of 3212 segments from CHF class (BIDMC database) and 3920 segments of normal class (500 segments from Fantasia database and 3420 segments from MIT-BIH NSR database). The RBF kernel parameter value is varied from 0.1 to 1.5 with step size of 0.1 to find the kernel parameter which yields highest

classification accuracy. Accuracy versus kernel parameter values for BD set 1, set 2, and FD set using 500 samples of HRV signals with LS-SVM classifier is shown in Figure 4.1.

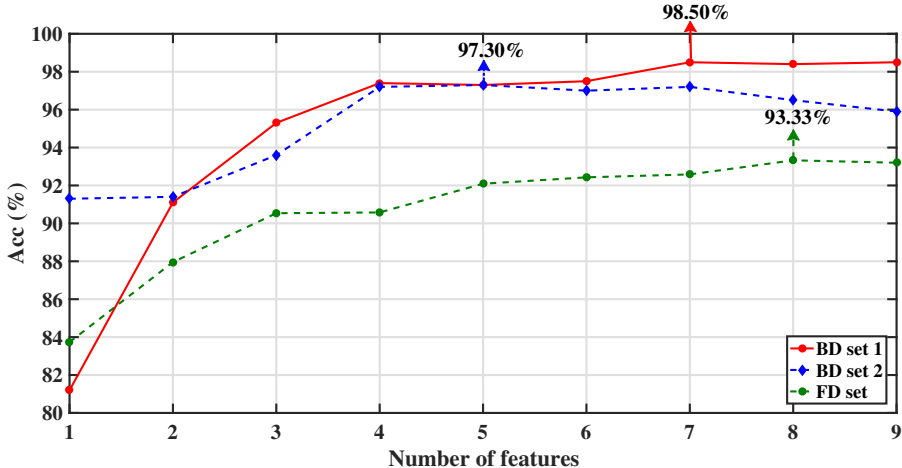


FIGURE 4.2: Accuracy versus number of features plot for BD set 1, set 2, and FD set using 500 samples of HRV signals with LS-SVM classifier.

4.1.1.1 BD set 1

The mean and SD of features evaluated from the decomposed components are shown in Table 4.1. The t -values for features are computed to rank the features. It can be observed from the table that t -values are remarkably high for first seven features. Hence, these features are given as input to the LS-SVM classifier. For BD set 1, we obtained Acc of 98.50%, Sen of 97.80%, and Spe of 99.20% using only 7 features (Figure. 4.2).

4.1.1.2 BD set 2

The BD set 2 is formed using 500 segments of normal class (Fantasia database) and 500 segments from CHF class. The mean and SD with t -values of features computed

TABLE 4.1: Mean and SD values of ranked features with t-value for normal (MIT-BIH database) and CHF classes using 500 samples of HRV signals.

Features	MIT-BIH NSR (mean \pm SD)	BIDMC CHF (mean \pm SD)	t-value
mf_h	0.1468 \pm 0.1046	0.38 \pm 0.1274	30.36
kNN_l	-12.7695 \pm 1.4437	-14.6921 \pm 1.7767	27.24
Corr	0.7263 \pm 0.0825	0.8009 \pm 0.0693	23.65
kNN_h	-14.836 \pm 1.3633	-16.5324 \pm 2.0346	23.11
mt_l	0.7954 \pm 0.1444	0.6608 \pm 0.1323	23
st_l	0.0318 \pm 0.0455	0.0172 \pm 0.1465	8.74
st_h	0.0127 \pm 0.0411	0.0103 \pm 0.1187	5.53
mf_l	0.0027 \pm 0.0024	0.0028 \pm 0.002	2.2
mt_h	0 \pm 0.00037	-0.000006 \pm 0.0006	0.34

from the decomposed components are presented in Table 4.2. We can observe from Figure 4.2 that, maximum Acc of 97.3%, Sen of 97.6% and Spe of 97% is obtained using only 5 features.

4.1.1.3 FD set

The mean and SD with t -values of features computed from the decomposed components for FD set are presented in Table 4.3. The plot of accuracy versus number of features for BD set 1, set 2, and FD set using 500 samples of HRV signals with LS-SVM classifier is shown in Figure 4.2. It can be observed from this figure that

TABLE 4.2: Mean and SD values of ranked features with t-value for normal (Fantasia database) and CHF classes using 500 samples of HRV signals.

Features	FANTASIA (mean \pm SD)	BIDMC CHF (mean \pm SD)	t-value
mt_l	0.9902 \pm 0.1461	0.6598 \pm 0.1273	20.48
Corr	0.6127 \pm 0.0865	0.8008 \pm 0.0682	20.38
kNN_h	-16.4534 \pm 1.1304	-18.1683 \pm 1.8247	15.27
mf_h	0.0913 \pm 0.1267	0.2905 \pm 0.1893	12.66
st_h	0.0073 \pm 0.0052	0.0069 \pm 0.0413	7.27
kNN_l	-14.7209 \pm 1.0435	-15.4945 \pm 1.8141	3.17
mf_l	0.0008 \pm 0	0.001 \pm 0.0031	2.7
st_l	0.0184 \pm 0.0099	0.0178 \pm 0.0375	1.08
mt_h	0 \pm 0.00024	0.000003 \pm 0.0001	0.39

we have obtained the highest Acc of 93.33%, Sen of 91.41% and Spe of 94.90% using only 8 features.

4.1.2 HRV signals of length 2000 samples

A set of 980 segments from 58 normal subjects and 803 segments from 15 CHF subjects with each segment having length of 2000 samples are chosen. BD set 1 comprises of 125 segments from normal class (MIT-BIH NSR dataset) and 125 segments from CHF class. BD set 2 contains 125 segments belonging to normal class (Fantasia dataset) and 125 segments from CHF class. FD set consists of 803

TABLE 4.3: Mean and SD values of ranked features with t-value for normal (MIT-BIH NSR database and Fantasia database) and CHF classes using 500 samples of HRV signals.

Features	Normal (mean \pm SD)	BIDMC CHF (mean \pm SD)	t-value
mf_h	0.0905 \pm 0.1103	0.2905 \pm 0.1893	26.46
mt_l	0.8202 \pm 0.1541	0.6598 \pm 0.1273	24.07
Corr	0.712 \pm 0.0894	0.8008 \pm 0.0682	23.77
kNN_h	-16.3826 \pm 1.3399	-18.1683 \pm 1.8247	23.09
kNN_l	-14.0563 \pm 1.4106	-15.4945 \pm 1.8141	18.37
st_l	0.0312 \pm 0.0274	0.0178 \pm 0.0375	8.43
st_h	0.0100 \pm 0.0177	0.0069 \pm 0.0413	2
mf_l	0.0009 \pm 0.0016	0.0010 \pm 0.0031	0.8
mt_h	0 \pm 0.0002	0.000003 \pm 0.0001	0.19

segments belonging to CHF class and 980 segments from normal class (125 segments from Fantasia dataset and 855 segments from MIT-BIH NSR dataset). The plot of accuracy versus kernel parameter values for 2000 samples is shown in Figure 4.3.

4.1.3 BD set 1

The mean and SD of features evaluated from the decomposed components are shown in Table 4.4. Features are then ranked using t -values and then supplied as input to

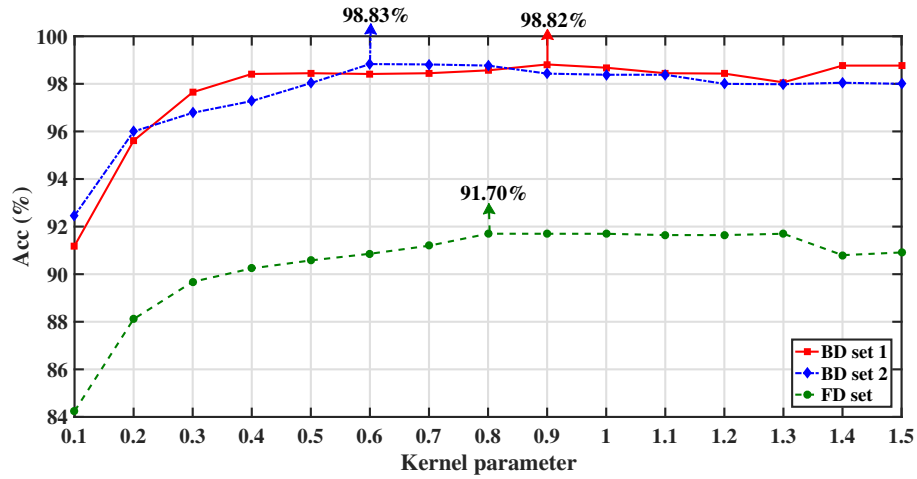


FIGURE 4.3: Accuracy versus kernel parameters for BD set 1, set 2, and FD set using 2000 samples of HRV signals with LS-SVM classifier.

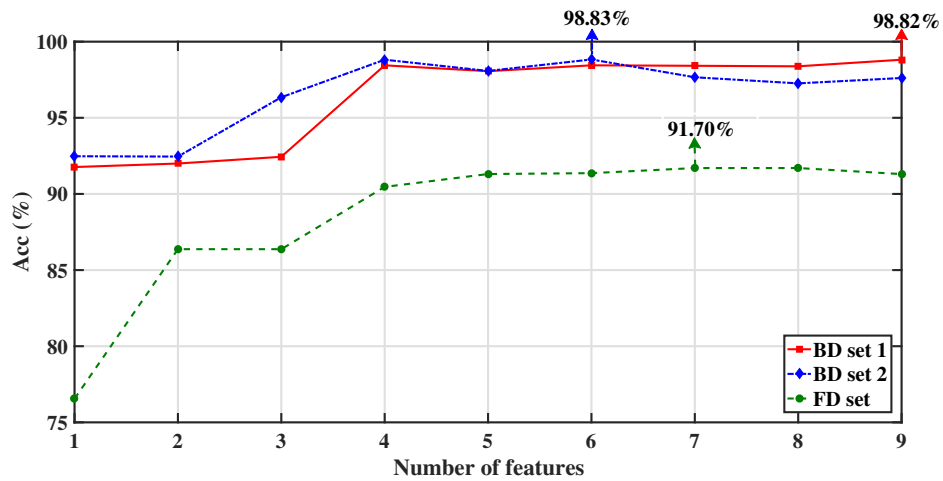


FIGURE 4.4: Accuracy versus number of features plot for BD set 1, set 2, and FD set using 2000 samples of HRV signals with LS-SVM classifier.

the LS-SVM classifier. We obtained a classification Acc of 98.82%, Sen of 99.23%, and Spe of 98.40% using only 9 features (Figure 4.4).

4.1.4 BD set 2

The BD set 2 is formed using 125 segments of normal class (Fantasia database) and 125 segments from CHF class. The mean and SD with t -values of features computed

TABLE 4.4: Mean and SD values of ranked features with t-value for normal (MIT-BIH database) and CHF classes using 2000 samples of HRV signals.

Features	MIT-BIH NSR (mean \pm SD)	BIDMC CHF (mean \pm SD)	t-value
kNN_h	-16.3722 \pm 1.3682	-18.1683 \pm 1.8247	17.08
Corr	0.7265 \pm 0.0802	0.8008 \pm 0.0682	12.39
mt_l	0.7954 \pm 0.1388	0.6598 \pm 0.1273	12.37
mf_h	0.0904 \pm 0.1078	0.2905 \pm 0.1893	10.67
kNN_l	-13.9592 \pm 1.4314	-15.4945 \pm 1.8141	8.71
st_l	0.0331 \pm 0.0286	0.0178 \pm 0.0375	6.21
st_h	0.0104 \pm 0.0188	0.0069 \pm 0.0413	4.68
mf_l	0.0009 \pm 0.0017	0.001 \pm 0.0031	1.61
mt_h	0 \pm 0.00019	0.000003 \pm 0.0001	0.8

from the decomposed components are presented in Table 4.5. We can observe from Figure 4.4 that, maximum Acc of 98.83%, Sen of 98.33% and Spe of 99.23% is achieved using only 6 features.

4.1.5 FD set

The mean and SD together with t -values of features computed from the decomposed components for FD set are presented in Table 4.6. The plot of accuracy versus number of features for BD set 1, set 2, and FD set from 2000 samples of HRV signals with LS-SVM classifier is shown in Figure 4.4. It can be observed from this

TABLE 4.5: Mean and SD values of ranked features with t-value for normal (Fantasia database) and CHF classes using 2000 samples o HRV signals.

Features	FANTASIA (mean \pm SD)	BIDMC CHF (mean \pm SD)	t-value
mt_l	0.9902 \pm 0.1461	0.6598 \pm 0.1273	20.48
Corr	0.6127 \pm 0.0865	0.8008 \pm 0.0682	20.38
kNN_h	-16.4534 \pm 1.1304	-18.1683 \pm 1.8247	15.27
mf_h	0.0913 \pm 0.1267	0.2905 \pm 0.1893	12.66
st_h	0.0073 \pm 0.0052	0.0069 \pm 0.0413	7.27
kNN_l	-14.7209 \pm 1.0435	-15.4945 \pm 1.8141	3.17
mf_l	0.0008 \pm 0	0.0010 \pm 0.0031	2.7
st_l	0.0184 \pm 0.0099	0.0178 \pm 0.0375	1.08
mt_h	0 \pm 0.00024	0.000003 \pm 0.0001	0.39

figure that we have obtained the highest Acc of 91.70%, Sen of 88.68% and Spe of 94.18% using only 7 features.

4.2 Discussion

In the present technique, the HRV signals are decomposed using EVDHM method. The obtained LFC and HFC decomposed components are used for feature extraction. Mean and SD of the signal, mean frequency using FB series expansion are measured to use them as features for the classification of CHF and normal HRV signals. The

TABLE 4.6: Mean and SD values of ranked features with t-value for normal (MIT-BIH NSR database and Fantasia database) and CHF classes using 2000 samples of HRV signals

Features	Normal (mean \pm SD)	BIDMC CHF (mean \pm SD)	t-value
mf_h	0.0905 \pm 0.1103	0.2905 \pm 0.1893	26.46
mt_l	0.8202 \pm 0.1541	0.6598 \pm 0.1273	24.07
Corr	0.7120 \pm 0.0894	0.8008 \pm 0.0682	23.77
kNN_h	-16.3826 \pm 1.3399	-18.1683 \pm 1.8247	23.09
kNN_l	-14.0563 \pm 1.4106	-15.4945 \pm 1.8141	18.37
st_l	0.0312 \pm 0.0274	0.0178 \pm 0.0375	8.43
st_h	0.0100 \pm 0.0177	0.0069 \pm 0.0413	2
mf_l	0.0009 \pm 0.0016	0.0010 \pm 0.0031	0.8
mt_h	0 \pm 0.0002	0.000003 \pm 0.0001	0.19

kNN entropy for LFC and HFC and Corr between LFC and HFC are also evaluated. Study is performed on three combinations of data namely, BD set 1, BD set 2 and FD set for 500 and 2000 samples lengths. Three combinations for two different segment lengths are considered to evaluate the variation in the performance of the proposed methodology.

We have obtained the LFC and HFC of HRV signals using EVDHM method. The LFC in this work depicts the slow variation in the time series and the HFC represents the transient behaviour of signal.

We have used mean, deviation using mt , st and mf features to distinguish the signal

on the basis of LFC and HFC. The obtained LFC has lower value of mt feature for CHF HRV signal as compared to normal HRV signal in all combinations of datasets. The mt_l and mf_h features are ranked high and contributed significantly for the classification. The values of kNN entropy based features show lower value for CHF HRV signal as compared to the normal HRV signal. Similar results are obtained in [16] for CHF patient as compared to normal person. The correlation between LFC and HFC is measured by Corr. The Corr based feature holds high value for CHF HRV signal as compared to normal HRV signal in all combinations of our study. During CHF, the HRV decreases due to reduced pumping ability of myocardium resulting in high correlation and low entropy values.

In [59], CHF HRV signals are classified using 16 features with an accuracy of 98.79% for a data length of 2000 samples. While, authors obtained classification accuracy of 91.56% using 27 features from long-term HRV signal in [58]. The CHF detection from long-term HRV signal is time consuming and hence faster diagnosis may not be possible, which is required to alert the clinicians to provide further treatment. Therefore, we have studied the short-term HRV signals of length 500 samples for CHF diagnosis. Our method successfully obtained an accuracy of 98.50% with 7 features using 500 samples of HRV signals for BD set 1. In [97], authors obtained an accuracy of 98.40% using 11 features for BD set 1. The proposed methodology achieved an accuracy of 93.33% with 8 features for FD set using 500 samples of HRV signals. We have used 2000 samples of HRV signals and obtained an accuracy of 98.82% with 9 features. The authors in [16] obtained an accuracy of 96.70% using 12 features and in [97] an accuracy of 98.80% is achieved using 9 features for 2000 samples of HRV signals. Our proposed method uses less number of features to attain high accuracy as compared to [16] and [97] for CHF diagnosis using short term HRV signals. A summary of the developed methodologies in the literature and proposed methodology with studied databases and achieved performance measures

have been shown in Table 4.7. We have used one iteration in EVDHM to obtain the decomposed components and few features are used for classification with less computational complexity as compared to [16]. Therefore, our methodology has achieved good performance with less number of features and helps to diagnose the CHF efficiently using few features. This method uses Hankel matrix to decompose the multi-component non-stationary signal. The proposed technique may take more time to decompose long duration HRV signals.

TABLE 4.7: Summary of automated diagnosis of CHF using HRV signals.

Authors and year	Dataset and subjects	Methods	Signal length/ duration	Number of features	Performance measures
Jong et al. (2011) [41]	Normal- NSR RR interval (54) CHF - CHF RR interval (29)	DFA based sliding window analysis, SVM	24 hours	-	Acc= 96%, Sen= 87.00%, Spe= 100%
Yu et al. (2012) [59]	Normal- NSR RR interval (54) CHF - CHF RR interval (29)	Bispectral analysis (BSA), time and frequency domain based features, SVM	24 hours	16	Acc= 98.79%, Sen= 96.55%, Spe= 100%
Narin et al. (2014) [58]	Normal- NSR RR interval (54) CHF - CHF RR interval (29)	time and frequency domain measures, DFA, Poincare plot, sample entropy, SVM	24 hours	27	Acc= 91.56%, Sen= 82.75%, Spe= 96.29%
Acharya et al. (2016) [16]	Normal- MIT-BIH NSR (40) - Fantasia (18) CHF - BIDMC CHF (15)	Empirical mode decomposition (EMD), Renyi entropy, Shannon entropy and 11 other features, SVM	2000 samples 2000 samples	12 11	BD Set 1, Acc 96.70%, Sen= 98.40%, Spe= 95.20% BD Set 2, Acc =94.00%, Sen= 94.00%, Spe= 93.60%
Kumar et al. (2017) [97]	Normal- MIT-BIH NSR (40) - Fantasia (18) CHF - BIDMC CHF (15)	FAWT, permutation entropy, fuzzy entropy, LS-SVM	500 samples 500 samples	11 15	BD Set 1, Acc= 98.40%, Sen= 99.00%, Spe= 97.80% BD Set 2, Acc= 97.00%, Sen= 97.60%, Spe= 96.40%
Proposed work	Normal- MIT-BIH NSR (40) - Fantasia (18) CHF - BIDMC CHF (15)	EVDHM, coreentropy, kNN entropy, mean, SD, LS-SVM	500 samples 500 samples 500 samples	7 5 8	BD set 1, Acc= 98.50%, Sen= 97.80%, Spe= 99.20% BD set 2, Acc= 97.30%, Sen= 97.40%, Spe= 97% FD set, Acc= 93.33%, Sen= 91.41%, Spe= 94.90%

4.3 Summary

The HRV signals with segment size of 500 samples and 2000 samples are separately processed for two different combinations of data set, BD set 1 and BD set 2, and FD set. All the features corresponding to parameters, correntropy, kNN entropy, mt_l and mf_h are present in the first five ranked features that help in the classification of two classes, CHF and normal, with highest accuracy. Kernel parameter of LS-SVM classifier is varied from 0.1 to 1.5 and for the 500 samples length of HRV signals BD set 1, BD set 2 and FD set achieve the highest accuracy at kernel parameter value of 0.9, 1.3 and 0.7, respectively. In the case of 2000 samples length, it achieves the highest accuracy at kernel parameter value of 0.9, 0.6 and 0.8 respectively. The comparison of the proposed method has been done with the existing methods in the literature which shows that the classification accuracy obtained under this work are better than that obtained in previous works.

The number of features required to obtain these accuracy levels are also less for BD set 1 and BD set 2. For FD set, which has not been studied before as per our knowledge also achieves a decent accuracy level.

Chapter 5

Conclusion and Future Work

This work presents a novel technique for the automated diagnosis of CHF patients using HRV signals. The EVDHM method is used to decompose the HRV signals and HFC and LFC components are subsequently extracted. These HFC and LFC components contain the unique and relevant information of the CHF and normal HRV signals. Both linear and nonlinear features were extracted from these components and our methodology performed well for all three data sets (BD set 1, BD set 2 and FD set). We studied these features for two different signal lengths (2000 and 500 samples per segment) of HRV signals and tested our methodology on three different combinations of dataset. The proposed method is able to capture subtle variations efficiently and yielded the highest classification accuracy as compared to other existing methods. Our methodology performed well for all three combinations of dataset with classification accuracy, sensitivity and specificity of 93.33%, 91.41% and 94.90% respectively for combined full dataset of 500 samples length. Balanced dataset with 500 samples length achieved classification accuracy, sensitivity and specificity of 98.50%, 97.80% and 99.20% respectively. As this method provides better classification results even for short term HRV signals (signal length

of 500 samples), clinicians may find it useful for the timely correct diagnosis of CHF patients and also this may create a desire to work on noninvasive technique based on HRV signals to design a single cardiac test for the cardiac patients.

With good classification results, our findings also support the fact that HRV signals contain the relevant information of cardiac movements. In this work, we have used only 15 CHF patients for our study. In future, we intend to test our developed system using more patients from diverse background. We will also explore the selection criteria of the proposed decomposed technique and study different features which could help in faster and better classification. It would be of interest to explore the possibility of using our proposed method to diagnose other cardiac diseases like myocardial infarction, coronary artery disease and heart valve problems.

Bibliography

- [1] R. M. Anderson, *The Gross Physiology of the Cardiovascular System*. Robert M. Anderson, 1993.
- [2] N. D. Wong, “Epidemiological studies of CHD and the evolution of preventive cardiology,” *Nature Reviews Cardiology*, vol. 11, no. 5, pp. 276–289, 2014.
- [3] C. Starr, C. Evers, and L. Starr, *Biology Today and Tomorrow with Physiology*. Cengage Learning, 2015.
- [4] S. Standring, *Gray’s Anatomy: the Anatomical Basis of Clinical Practice*. Elsevier Health Sciences, 2015.
- [5] J.-P. Montani, J. F. Carroll, T. M. Dwyer, V. Antic, Z. Yang, and A. G. Dulloo, “Ectopic fat storage in heart, blood vessels and kidneys in the pathogenesis of cardiovascular diseases,” *International Journal of Obesity*, vol. 28, pp. S58–S65, 2004.
- [6] A. Anogeianaki, D. Angelucci, E. Cianchetti, M. D’alessandro, G. Maccauro, A. Saggini, V. Salini, A. Caraffa, S. Tete, F. Conti *et al.*, “Atherosclerosis: a classic inflammatory disease,” 2011.
- [7] U. R. Acharya, K. P. Joseph, N. Kannathal, C. M. Lim, and J. S. Suri, “Heart rate variability: a review,” *Medical and Biological Engineering and Computing*, vol. 44, no. 12, pp. 1031–1051, 2006.

- [8] T. A. Nappholz, A. K. Dawson, R. M. Lu, and B. M. Steinhaus, “Apparatus and method for detecting abnormal cardiac rhythms using evoked potential measurements in an arrhythmia control system,” Feb. 9 1993, US Patent 5,184,615.
- [9] F. Dal Pan, G. Donzella, C. Fucci, and M. Schreiber, “Structural effects of an innovative surgical technique to repair heart valve defects,” *Journal of Biomechanics*, vol. 38, no. 12, pp. 2460–2471, 2005.
- [10] P. Puska, S. Mendis, B. Norrving, W. H. Organization *et al.*, *Global Atlas on Cardiovascular Disease Prevention and Control*. Geneva: World Health Organization, 2011.
- [11] M. H. Drazner, J. E. Rame, L. W. Stevenson, and D. L. Dries, “Prognostic importance of elevated jugular venous pressure and a third heart sound in patients with heart failure,” *New England Journal of Medicine*, vol. 345, no. 8, pp. 574–581, 2001.
- [12] G. A. Holzapfel and R. W. Ogden, *Biomechanics of Soft Tissue in Cardiovascular Systems*. Springer, 2014, vol. 441.
- [13] M. R. Zile and D. L. Brutsaert, “New concepts in diastolic dysfunction and diastolic heart failure: part I,” *Circulation*, vol. 105, no. 11, pp. 1387–1393, 2002.
- [14] C. W. Yancy, M. Jessup, B. Bozkurt, J. Butler, D. E. Casey, M. H. Drazner, G. C. Fonarow, S. A. Geraci, T. Horwich, J. L. Januzzi, *et al.*, “2013 ACCF/AHA guideline for the management of heart failure,” *Circulation*, pp. CIR-0b013e31 829e8776, 2013.
- [15] P. Pazos-López, J. Peteiro-Vázquez, A. Carcía-Campos, L. García-Bueno, J. P. A. de Torres, and A. Castro-Beiras, “The causes, consequences, and

treatment of left or right heart failure,” *Vascular Health and Risk Management*, vol. 7, pp. 237–254, 2011.

- [16] U. R. Acharya, H. Fujita, V. K. Sudarshan, S. Lih Oh, A. Muhammad, J. E. W. Koh, J. Hong Tan, C. K. Chua, K. Poo Chua, and R. San Tan, “Application of empirical mode decomposition (EMD) for automated identification of congestive heart failure using heart rate signals,” *Neural Computing and Applications*, vol. 22, p. 1250027, 2016.
- [17] J. J. McMurray, S. Adamopoulos, S. D. Anker, A. Auricchio, M. Böhm, K. Dickstein, V. Falk, G. Filippatos, C. Fonseca, M. A. Gomez-Sanchez *et al.*, “ESC guidelines for the diagnosis and treatment of acute and chronic heart failure 2012,” *European Journal of Heart Failure*, vol. 14, no. 8, pp. 803–869, 2012.
- [18] T. Gotoh, T. Kuroda, M. Yamasawa, M. Nishinaga, T. Mitsuhashi, Y. Seino, N. Nagoh, K. Kayaba, S. Yamada, H. Matsuo *et al.*, “Correlation between lipoprotein (a) and aortic valve sclerosis assessed by echocardiography (the JMS cardiac echo and cohort study),” *The American Journal of Cardiology*, vol. 76, no. 12, pp. 928–932, 1995.
- [19] M. M. Redfield, S. J. Jacobsen, J. C. Burnett Jr, D. W. Mahoney, K. R. Bailey, and R. J. Rodeheffer, “Burden of systolic and diastolic ventricular dysfunction in the community: appreciating the scope of the heart failure epidemic,” *JAMA*, vol. 289, no. 2, pp. 194–202, 2003.
- [20] M. Brodsky, D. Wu, P. Denes, C. Kanakis, and K. M. Rosen, “Arrhythmias documented by 24 hour continuous electrocardiographic monitoring in 50 male medical students without apparent heart disease,” *The American Journal of Cardiology*, vol. 39, no. 3, pp. 390–395, 1977.

- [21] M. Bolanos, H. Nazeran, and E. Haltiwanger, "Comparison of heart rate variability signal features derived from electrocardiography and photoplethysmography in healthy individuals," in *2006 International Conference of the IEEE Engineering in Medicine and Biology Society*, New York, pp. 4289–4294, 2006.
- [22] K. Chua, V. Chandran, U. Acharya, and C. Lim, "Cardiac state diagnosis using higher order spectra of heart rate variability," *Journal of Medical Engineering & Technology*, vol. 32, no. 2, pp. 145–155, 2008.
- [23] L. Sörnmo and P. Laguna, *Bioelectrical Signal Processing in Cardiac and Neurological Applications*, Academic Press, vol. 8, 2005,
- [24] T. Bolton, "Mechanisms of action of transmitters and other substances on smooth muscle." *Physiological Reviews*, vol. 59, no. 3, pp. 606–718, 1979.
- [25] T. B. Kinraide and B. Etherton, "Energy coupling in h⁺-amino acid cotransport ATP dependence of the spontaneous electrical repolarization of the cell membranes in oat coleoptiles," *Plant Physiology*, vol. 69, no. 3, pp. 648–652, 1982.
- [26] L. Biel, O. Pettersson, L. Philipson, and P. Wide, "ECG analysis: a new approach in human identification," *IEEE Transactions on Instrumentation and Measurement*, vol. 50, no. 3, pp. 808–812, 2001.
- [27] A. L. Goldberger, L. A. Amaral, L. Glass, J. M. Hausdorff, P. C. Ivanov, R. G. Mark, J. E. Mietus, G. B. Moody, C. K. Peng, and H. E. Stanley, "Physiobank, physiotoolkit, and physionet components of a new research resource for complex physiologic signals," *Circulation*, vol. 101, no. 23, pp. e215–e220, 2000.
- [28] A. S. Khaled, M. I. Owis, and A. S. A. Mohamed, "Employing time-domain methods and Poincare plot of heart rate variability signals to detect congestive heart failure," *BIME Journal*, vol. 6, no. 1, pp. 35–41, 2006.

- [29] S. B. Donald, S. C. Wilson, E. S. Monrad, S. S. Harton, F. W. Richard, L. Alyce, F. G. Diane, J. R. Bernard, G. William, and B. Eugene, "Survival of patients with severe congestive heart failure treated with oral milrinone," *Journal of the American College of Cardiology*, vol. 7, no. 3, pp. 661–670, 1986.
- [30] D. Giri, U. R. Acharya, R. J. Martis, S. V. Sree, T. C. Lim, T. Ahamed VI, and J. S. Suri, "Automated diagnosis of coronary artery disease affected patients using LDA, PCA, ICA and discrete wavelet transform," *Knowledge-Based Systems*, vol. 37, pp. 274–282, 2013.
- [31] S. Patidar, R. B. Pachori, and U. R. Acharya, "Automated diagnosis of coronary artery disease using tunable-Q wavelet transform applied on heart rate signals," *Knowledge-Based Systems*, vol. 82, pp. 1–10, 2015.
- [32] M. Kumar, R. B. Pachori, and U. R. Acharya, "An efficient automated technique for CAD diagnosis using flexible analytic wavelet transform and entropy features extracted from HRV signals," *Expert Systems with Applications*, vol. 63, pp. 165–172, 2016.
- [33] S. Sood, M. Kumar, R. B. Pachori, and U. R. Acharya, "Application of empirical mode decomposition-based features for analysis of normal and CAD heart rate signals," *Journal of Mechanics in Medicine and Biology*, vol. 16(1), no. 1, p. 1640002, 2016.
- [34] U. R. Acharya, K. S. Vidya, D. N. Ghista, W. J. E. Lim, F. Molinari, and S. Meena, "Computer-aided diagnosis of diabetic subjects by heart rate variability signals using discrete wavelet transform method," *Knowledge-Based Systems*, vol. 81, pp. 56–64, 2015.
- [35] R. B. Pachori, A. Pakala, K. Shashank, R. Sharma, and U. R. Acharya, "Application of empirical mode decomposition for analysis of normal and diabetic

- RR-interval signals,” *Expert Systems with Applications*, vol. 42, no. 9, pp. 4567–4581, 2015.
- [36] R. B. Pachori, M. Kumar, P. Avinash, K. Shashank, and U. R. Acharya, “An improved online paradigm for screening of diabetic patients using RR-interval signals,” *Journal of Mechanics in Medicine and Biology*, vol. 16, no. 01, p. 1640003, 2016.
- [37] H. Mussalo, E. Vanninen, R. Ikäheimo, T. Laitinen, M. Laakso, E. Länsimies, and J. Hartikainen, “Heart rate variability and its determinants in patients with severe or mild essential hypertension,” *Clinical Physiology*, vol. 21, no. 5, pp. 594–604, 2001.
- [38] J. Nolan, P. D. Batin, R. Andrews, S. J. Lindsay, P. Brooksby, M. Mullen, W. Baig, A. D. Flapan, A. Cowley, R. J. Prescott, J. M. M. Neilson, and K. A. A. Fox, “Prospective study of heart rate variability and mortality in chronic heart failure,” *Circulation*, vol. 98, no. 15, pp. 1510–1516, 1998.
- [39] M. Hadase, A. Azuma, K. Zen, S. Asada, T. Kawasaki, T. Kamitani, S. Kawasaki, H. Sugihara, and H. Matsubara, “Very low frequency power of heart rate variability is a powerful predictor of clinical prognosis in patients with congestive heart failure,” *Circulation Journal*, vol. 68, no. 4, pp. 343–347, 2004.
- [40] T. P. Thakre and M. L. Smith, “Loss of lag-response curvilinearity of indices of heart rate variability in congestive heart failure,” *BMC Cardiovascular Disorders*, vol. 6, no. 1, p. 27, 2006.
- [41] T. L. Jong, B. Chang, and C. D. Kuo, “Optimal timing in screening patients with congestive heart failure and healthy subjects during circadian observation,” *Annals of Biomedical Engineering*, vol. 39, no. 2, pp. 835–849, 2011.

- [42] P. Melillo, R. Fusco, M. Sansone, M. Bracale, and L. Pecchia, "Discrimination power of long-term heart rate variability measures for chronic heart failure detection," *Medical and Biological Engineering and Computing*, vol. 49, no. 1, pp. 67–74, 2011.
- [43] R. Maestri, G. D. Pinna, A. Accardo, P. Allegrini, R. Balocchi, G. D'addio, M. Ferrario, D. Menicucci, A. Porta, R. Sassi, M. G. Signorini, M. T. La Rovere, and S. Cerutti, "Nonlinear indices of heart rate variability in chronic heart failure patients: Redundancy and comparative clinical value," *Journal of Cardiovascular Electrophysiology*, vol. 18, no. 4, pp. 425–433, 2007.
- [44] F. Shahbazi and B. M. Asl, "Generalized discriminant analysis for congestive heart failure risk assessment based on long-term heart rate variability," *Computer Methods and Programs in Biomedicine*, vol. 122, no. 2, pp. 191–198, 2015.
- [45] J. O. Mudd and D. A. Kass, "Tackling heart failure in the twenty-first century," *Nature*, vol. 451, no. 7181, pp. 919–928, 2008.
- [46] P. Jain and R. B. Pachori, "An iterative approach for decomposition of multi-component non-stationary signals based on eigenvalue decomposition of the Hankel matrix," *Journal of the Franklin Institute*, vol. 352, no. 10, pp. 4017–4044, 2015.
- [47] P. Jain and R. B. Pachori, "GCI identification from voiced speech using the eigen value decomposition of Hankel matrix," in *2013 8th International Symposium on Image and Signal Processing and Analysis (ISPA)*, pp. 371–376, 2013.

- [48] P. Jain and R. B. Pachori, “Event-based method for instantaneous fundamental frequency estimation from voiced speech based on eigenvalue decomposition of the Hankel matrix,” *IEEE/ACM Transactions on Audio, Speech and Language Processing*, vol. 22, no. 10, pp. 1467–1482, 2014.
- [49] R. R. Sharma and R. B. Pachori, “A new method for non-stationary signal analysis using eigenvalue decomposition of the Hankel matrix and Hilbert transform,” *Fourth International Conference on Signal Processing and Integrated Networks (SPIN 2017)*, 2-3 Feb, 2017.
- [50] J. Shi and J. Malik, “Normalized cuts and image segmentation,” *IEEE Transactions on Pattern Analysis and Machine Intelligence*, vol. 22, no. 8, pp. 888–905, 2000.
- [51] S. Wold, K. Esbensen, and P. Geladi, “Principal component analysis,” *Chemometrics and Intelligent Laboratory Systems*, vol. 2, no. 1-3, pp. 37–52, 1987.
- [52] A. N. Langville and C. D. Meyer, “A survey of eigenvector methods for web information retrieval,” *SIAM Review*, vol. 47, no. 1, pp. 135–161, 2005.
- [53] G. Strang and G. Strang, *Linear Algebra and its Applications*, 1976, no. 04; QA184, S8.
- [54] E. Kreyszig, E. Kreyszig, and E. J. Norminton, *Advanced Engineering Mathematics*. John Wiley New York, 2006, vol. 72.
- [55] J. Gilbert and L. Gilbert, *Linear Algebra and Matrix Theory*. Academic Press, 2014.
- [56] A. L. Rukhin, “Analysis of time series structure SSA and related techniques,” 2002.

- [57] N. Iyengar, C. K. Peng, R. Morin, A. L. Goldberger, and L. A. Lipsitz, “Age-related alterations in the fractal scaling of cardiac interbeat interval dynamics,” *American Journal of Physiology-Regulatory, Integrative and Comparative Physiology*, vol. 271, no. 4, pp. R1078–R1084, 1996.
- [58] N. Ali, I. Yalcin, and O. Mahmut, “Investigating the performance improvement of HRV indices in CHF using feature selection methods based on backward elimination and statistical significance,” *Computers in Biology and Medicine*, vol. 45, pp. 72–79, 2014.
- [59] S. N. Yu and M. Y. Lee, “Bispectral analysis and genetic algorithm for congestive heart failure recognition based on heart rate variability,” *Computers in Biology and Medicine*, vol. 42, no. 8, pp. 816–825, 2012.
- [60] A. Kraskov, H. Stogbauer, and P. Grassberger, “Estimating mutual information,” *Physical Review E*, vol. 69, no. 6, p. 066138, 2004.
- [61] W. Liu, P. P. Pokharel, and J. C. Príncipe, “Correntropy: Properties and applications in non-Gaussian signal processing,” *IEEE Transactions on Signal Processing*, vol. 55, no. 11, pp. 5286–5298, 2007.
- [62] R. B. Pachori, and P. Sircar, , “Analysis of multicomponent AM-FM signals using FB-DESA method,” *Digital Signal Processing*, vol. 20, no. 1, pp. 42–62, 2010.
- [63] R. B. Pachori, and P. Sircar, , “A new technique to reduce cross terms in the Wigner distribution,” *Digital Signal Processing*, vol. 17, no. 2, pp. 466 - 474, 2007.
- [64] J. Schroeder, “Signal processing via Fourier-Bessel series expansion,” *Digital Signal Processing*, vol. 3, no. 2, pp. 112–124, 1993.

- [65] R. B. Pachori, D. Hewson, H. Snoussi, and J. Duchêne, “Analysis of center of pressure signals using empirical mode decomposition and Fourier-Bessel expansion,” *IEEE Region 10 TENCON Conf.*, Hyderabad, pp. 1–6, 2008.
- [66] R. B. Pachori and P. Sircar, “Speech analysis using Fourier-Bessel expansion and discrete energy separation algorithm,” *IEEE 12th Digital Signal Processing Workshop & 4th IEEE Signal Processing Education Workshop*, pp. 423–428, 2006.
- [67] R. B. Pachori, “Discrimination between ictal and seizure-free EEG signals using empirical mode decomposition,” *Research Letters in Signal Processing*, vol. 2008, p. 14, 2008.
- [68] R. B. Pachori, “EEG signal analysis using FB expansion and second-order linear TVAR process,” *Signal Processing*, vol. 88, no. 2, p. 415-420, 2008.
- [69] Y. Mack and M. Rosenblatt, “Multivariate k-nearest neighbor density estimates,” *Journal of Multivariate Analysis*, vol. 9, no. 1, pp. 1–15, 1979.
- [70] N. S. Altman, “An introduction to kernel and nearest-neighbor nonparametric regression,” *The American Statistician*, vol. 46, no. 3, pp. 175–185, 1992.
- [71] K. A. Veselkov, V. I. Pahomov, J. C. Lindon, V. S. Volynkin, D. Crockford, G. S. Osipenko, D. B. Davies, R. H. Barton, J. W. Bang, E. Holmes, et al., “A metabolic entropy approach for measurements of systemic metabolic disruptions in patho-physiological states,” *Journal of Proteome Research*, vol. 9, no. 7, pp. 3537–3544, 2010.
- [72] I. Santamaría, P. P. Pokharel, and J. C. Principe, “Generalized correlation function: definition, properties, and application to blind equalization,” *IEEE Transactions on Signal Processing*, vol. 54, no. 6, pp. 2187–2197, 2006.

- [73] H. Yan, X. Yuan, S. Yan, and J. Yang, “Correntropy based feature selection using binary projection,” *Pattern Recognition*, vol. 44, no. 12, pp. 2834–2842, 2011.
- [74] A. Singh and J. C. Principe, “Using correntropy as a cost function in linear adaptive filters,” *2009. International Joint Conference on Neural Networks, Atlanta, GA*, pp. 2950–2955, 2009.
- [75] J.-W. Xu, H. Bakardjian, A. Cichocki, and J. C. Principe, “A new nonlinear similarity measure for multichannel signals,” *Neural Networks*, vol. 21, no. 2, pp. 222–231, 2008.
- [76] V. Gupta, T. Priya, A. K. Yadav, R. B. Pachori, and U. R. Acharya, “Automated detection of focal EEG signals using features extracted from flexible analytic wavelet transform,” *Pattern Recognition Letters*, vol. 94, pp. 180 – 188, 2017.
- [77] S. Maheshwari, R. B. Pachori, and U. R. Acharya, “Automated diagnosis of glaucoma using empirical wavelet transform and correntropy features extracted from fundus images,” *IEEE Journal of Biomedical and Health Informatics*, vol. 21, no. 3, pp. 803–813, 2017.
- [78] X. Liu, J. Shi, S. Zhou, and M. Lu, “An iterated laplacian based semi-supervised dimensionality reduction for classification of breast cancer on ultrasound images,” in *2014 36th Annual International Conference of the IEEE Engineering in Medicine and Biology Society*, Aug 2014, pp. 4679–4682.
- [79] E. Hasanbelliu, J. Principe, and C. Slatton, “Correntropy based matched filtering for classification in sidescan sonar imagery,” *2009 IEEE International Conference on Systems, Man and Cybernetics*, San Antonio, pp. 2757–2762, 2009.

- [80] R. O. Duda, P. E. Hart, and D. G. Stork, *Pattern Classification*. John Wiley & Sons, 2012.
- [81] R. Sharma, R. B. Pachori, and U. R. Acharya, “An integrated index for the identification of focal electroencephalogram signals using discrete wavelet transform and entropy measures,” *Entropy*, vol. 17, no. 8, pp. 5218–5240, 2015.
- [82] S. Aksoy and R. M. Haralick, “Feature normalization and likelihood-based similarity measures for image retrieval,” *Pattern Recognition Letters*, vol. 22, no. 5, pp. 563–582, 2001.
- [83] M. H. Dunham, *Data Mining: Introductory and Advanced Topics*. Pearson Education India, 2006.
- [84] J. A. K. Suykens and J. Vandewalle, “Least squares support vector machine classifiers,” *Neural Processing Letters*, vol. 9, no. 3, pp. 293–300, 1999.
- [85] S. Zheng, W. Z. Shi, J. Liu, and J. Tian, “Remote sensing image fusion using multiscale mapped LS-SVM,” *IEEE Transactions on Geoscience and Remote Sensing*, vol. 46, no. 5, pp. 1313–1322, 2008.
- [86] V. Mitra, C. J. Wang, and S. Banerjee, “Text classification: A least square support vector machine approach,” *Applied Soft Computing*, vol. 7, no. 3, pp. 908–914, 2007.
- [87] M. M. Adankon and M. Cheriet, “Model selection for the LS-SVM. Application to handwriting recognition,” *Pattern Recognition*, vol. 42, no. 12, pp. 3264–3270, 2009.
- [88] Z. Yan, Z. Wang, and H. Xie, “The application of mutual information-based feature selection and fuzzy LS-SVM based classifier in motion classification,” *Computer Methods and Programs in Biomedicine*, vol. 90, no. 3, pp. 275–284, 2008.

- [89] R. Sharma, R. B. Pachori, and U. R. Acharya, "Application of entropy measures on intrinsic mode functions for the automated identification of focal electroencephalogram signals," *Entropy*, vol. 17(2), no. 2, pp. 669–691, 2015.
- [90] V. Bajaj and R. B. Pachori, "Classification of seizure and nonseizure EEG signals using empirical mode decomposition," *IEEE Transactions on Information Technology in Biomedicine*, vol. 16, no. 6, pp. 1135–1142, 2012.
- [91] V. Bajaj and R. B. Pachori, "EEG signal classification using empirical mode decomposition and support vector machine," in *Proceedings of the International Conference on Soft Computing for Problem Solving (SocProS 2011) December 20-22, 2011*. Springer, 2012, pp. 623–635.
- [92] R. Sharma and R. B. Pachori, "Classification of epileptic seizures in EEG signals based on phase space representation of intrinsic mode functions," *Expert Systems with Applications*, vol. 42, no. 3, pp. 1106–1117, 2015.
- [93] R. B. Pachori and S. Patidar, "Epileptic seizure classification in EEG signals using second-order difference plot of intrinsic mode functions," *Computer Methods and Programs in Biomedicine*, vol. 113, no. 2, pp. 494–502, 2014.
- [94] U. Acharya, O. Faust, S. V. Sree, F. Molinari, R. Garberoglio, and J. Suri, "Cost-effective and non-invasive automated benign & malignant thyroid lesion classification in 3D contrast-enhanced ultrasound using combination of wavelets and textures: a class of ThyroScanTM algorithms," *Technology in Cancer Research & Treatment*, vol. 10, no. 4, p. 371380, 2011.
- [95] L. Wang, *Support Vector Machines: Theory and Applications*. Springer Science & Business Media, 2005, vol. 177.

- [96] M. Kumar, R. B. Pachori, and U. R. Acharya, "Characterization of coronary artery disease using flexible analytic wavelet transform applied on ECG signals," *Biomedical Signal Processing and Control*, vol. 31, pp. 301–308, 2017.
- [97] M. Kumar, R. B. Pachori, and U. R. Acharya, "Use of accumulated entropies for automated detection of congestive heart failure in flexible analytic wavelet transform framework based on short-term HRV signals," *Entropy*, vol. 19, no. 3, p. 92, 2017.
- [98] A. H. Khandoker, D. T. H. Lai, R. K. Begg, and M. Palaniswami, "Wavelet-based feature extraction for support vector machines for screening balance impairments in the elderly," *IEEE Transactions on Neural Systems and Rehabilitation Engineering*, vol. 15, no. 4, pp. 587–597, 2007.
- [99] R. Kohavi, "A study of cross-validation and bootstrap for accuracy estimation and model selection", *IJCAI*, vol. 14, no. 2, 1995.
- [100] A. T. Azar and S. A. El-Said, "Performance analysis of support vector machines classifiers in breast cancer mammography recognition," *Neural Computing and Applications*, vol. 24, no. 5, pp. 1163–1177, 2014.
- [101] J. A. Suykens, T. Van Gestel, and J. De Brabanter, *Least Squares Support Vector Machines*. World Scientific, 2002.
- [102] M. H. Asyali, "Discrimination power of long-term heart rate variability measures," in *Proceedings of the 25th Annual International Conference of the IEEE Engineering in Medicine and Biology Society*, vol. 1, pp. 200–203, 2003.
- [103] M. Sharma, R. B. Pachori, and U. R. Acharya, "A new approach to characterize epileptic seizures using analytic time-frequency flexible wavelet transform and fractal dimension," *Pattern Recognition Letters*, vol. 94, pp. 172 – 179, 2017.

- [104] R. Sharma, R. B. Pachori, and A. Upadhyay, "Automatic sleep stages classification based on iterative filtering of electroencephalogram signals," *Neural Computing and Applications*, pp. 1–20, 2017.
- [105] A. Bhattacharyya and R. B. Pachori, "A multivariate approach for patient specific EEG seizure detection using empirical wavelet transform," *IEEE Transactions on Biomedical Engineering*, vol. PP, no. 99, pp. 1–11, 2017.
- [106] A. Bhattacharyya, M. Sharma, R. B. Pachori, P. Sircar, and U. R. Acharya, "A novel approach for automated detection of focal EEG signals using empirical wavelet transform," *Neural Computing and Applications*, pp. 1–11, 2016.
- [107] R. Sharma, M. Kumar, R. B. Pachori, and U. R. Acharya, "Decision support system for focal EEG signals using tunable-Q wavelet transform," *Journal of Computational Science*, 2017.
- [108] A. Bhattacharyya, R. B. Pachori, A. Upadhyay, and U. R. Acharya, "Tunable-Q wavelet transform based multiscale entropy measure for automated classification of epileptic EEG signals," *Applied Sciences*, vol. 7, no. 4, p. 385, 2017.
- [109] A. Bhattacharyya, R. B. Pachori, and U. R. Acharya, "Tunable-Q wavelet transform based multivariate sub-band fuzzy entropy with application to focal EEG signal analysis," *Entropy*, vol. 19, no. 3, p. 99, 2017.
- [110] M. Sharma, A. Dhere, R. B. Pachori, and U. R. Acharya, "An automatic detection of focal EEG signals using new class of time-frequency localized orthogonal wavelet filter banks," *Knowledge-Based Systems*, vol. 118, pp. 217–227, 2017.
- [111] S. Patidar, R. B. Pachori, A. Upadhyay, and U. R. Acharya, "An integrated alcoholic index using tunable-Q wavelet transform based features extracted

- from EEG signals for diagnosis of alcoholism,” *Applied Soft Computing*, vol. 50, pp. 71–78, 2017.
- [112] M. Kumar, R. B. Pachori, and U. R. Acharya, “An efficient automated technique for CAD diagnosis using flexible analytic wavelet transform and entropy features extracted from HRV signals,” *Expert Systems with Applications*, vol. 63, pp. 165–172, 2016.
- [113] O. Sahu, V. Anand, V. Kanhangad, and R. B. Pachori, “Classification of magnetic resonance brain images using bi-dimensional empirical mode decomposition and autoregressive model,” *Biomedical Engineering Letters*, vol. 5, no. 4, pp. 311–320, 2015.
- [114] S. Patidar, R. B. Pachori, and U. R. Acharya, “Automated diagnosis of coronary artery disease using tunable-Q wavelet transform applied on heart rate signals,” *Knowledge-Based Systems*, vol. 82, pp. 1–10, 2015.
- [115] S. Patidar, R. B. Pachori, and N. Garg, “Automatic diagnosis of septal defects based on tunable-Q wavelet transform of cardiac sound signals,” *Expert Systems with Applications*, vol. 42, no. 7, pp. 3315–3326, 2015.
- [116] T. S. Kumar, V. Kanhangad, and R. B. Pachori, “Classification of seizure and seizure-free EEG signals using local binary patterns,” *Biomedical Signal Processing and Control*, vol. 15, pp. 33–40, 2015.
- [117] S. Patidar and R. B. Pachori, “Classification of cardiac sound signals using constrained tunable-Q wavelet transform,” *Expert Systems with Applications*, vol. 41, no. 16, pp. 7161–7170, 2014.
- [118] V. Joshi, R. B. Pachori, and A. Vijesh, “Classification of ictal and seizure-free EEG signals using fractional linear prediction,” *Biomedical Signal Processing and Control*, vol. 9, pp. 1–5, 2014.

- [119] V. Bajaj and R. B. Pachori, “Automatic classification of sleep stages based on the time-frequency image of EEG signals,” *Computer Methods and Programs in Biomedicine*, vol. 112, no. 3, pp. 320–328, 2013.
- [120] A. C. Guyton, “Textbook of medical physiology.” *Academic Medicine*, vol. 36, no. 5, p. 556, 1961.
- [121] K. A. Veselkov, V. I. Pahomov, J. C. Lindon, V. S. Volynkin, D. Crockford, G. S. Osipenko, D. B. Davies, R. H. Barton, J.-W. Bang, E. Holmes *et al.*, “A metabolic entropy approach for measurements of systemic metabolic disruptions in patho-physiological states,” *Journal of Proteome Research*, vol. 9, no. 7, pp. 3537–3544, 2010.